6 Understanding Clinical Flow Cytometry

Albert D. Donnenberg and Vera S. Donnenberg

CONTENTS

6.1 INTRODUCTION

One of the major advances in laboratory medicine has been the ability to immunologically identify specific subsets of leukocytes and other cells by their expression of proteins and other markers. This process, termed "immunophenotyping," employs monoclonal antibodies reactive against cell-associated determinants to distinguish specific subsets within a heterogeneous mixture of cells. Quantification of a subset of interest can be readily accomplished by the use of a *flow cytometer*, an instrument

that electronically measures the intensity of scattered or emitted light from individual cells as they pass before a laser.

In clinical laboratories, immunophenotyping by flow cytometry has been invaluable for defining the cell of origin of specific neoplasms, particularly in patients with acute leukemia or non-Hodgkin's lymphoma (see Chapter 7). A second major application is to provide information critical for the staging and management of human immunodeficiency virus (HIV)-1 infected patients and patients with other immune deficiency syndromes (see Chapters 8, 12 respectively); the data derived from analysis of T-cell subsets play an important role in guiding therapeutic decisions. A host of additional applications, including quantification of hematopoietic stem cells [1] and reticulocytes [2], diagnosis of acquired and congenital immune deficiency syndromes (see Chapter 9), paroxysmal nocturnal hemoglobinuria [3], detection of minimal residual leukemia after therapy [4], and many others are either approved as *in vitro* diagnostic (IVD) tests, or serve as diagnostic adjuncts to licensed tests. In addition to clinical considerations, these analytic techniques provide essential information concerning the structure and function of the cells comprising normal hematopoietic and lymphoid cells. In addition to the analysis of cells that occur naturally as single-cell suspensions (blood, lymph, bone marrow, cerebrospinal fluid, ascites, and effusions), flow cytometry can also be used to analyze marker expression and function in disaggregated tissue specimens. This review will focus on the factors that make cytometry as robust as it is, and also on avoiding the pitfalls inherent in such a flexible technique.

Flow cytometry is a mature clinical technique at present. When it was first introduced as a research tool a little more than 30 years ago, both instrumentation and analytical reagents were of limited usefulness [5]. The first instruments measured fluorescence on a linear scale at a single wavelength and displayed the values on an oscilloscope. The only means of recording and analyzing data was to make Polaroid photographs of the oscilloscope screen. Major advances in hardware and software spurred by the digital revolution, which together with the development of monoclonal antibodies and new dye technologies, have resulted in the emergence of instruments and procedures that are readily adaptable to clinical laboratories. Several publications are available that detail the principles of cytometry and the operation of flow cytometers [6–12].

6.2 MONOCLONAL ANTIBODIES

The invention of monoclonal antibodies by Milstein and colleagues in 1977 [13] changed the field of flow cytometry, providing an inexhaustible supply of reagents of exquisite specificity. By definition, a monoclonal antibody is an immunoglobulin produced by a clonal population of immortalized hybridoma cells. Accordingly, the antigen-binding sites are completely homogeneous, a situation very different from naturally occurring (polyclonal) antibodies. Because of their homogeneity, hybridomas can be selected which produce high-affinity antibodies with great specificity for particular antigenic determinants. Within a year of Milstein's invention, monoclonal antibodies specific for rat [14] and murine [15] helper T cells and murine MHC antigens [16] were described. Shortly thereafter, the description of three murine monoclonal antibodies specific for human T-cell surface determinants, designated OKT1,

OKT3, and OKT4 [17] paved the way for human studies. Today, these hybridomas are recognized as producing antibodies against the CD5, CD3, and CD4 determinants, respectively. Most of the monoclonal antibodies currently in use for the detection of determinants on human cells are of murine origin. The antibodies are generated to proteins, glycoproteins, glycolipids, and carbohydrates. The biological functions of these molecules are varied and include serving as membrane receptors or ligands for soluble and contact-dependent signaling, acting as enzymes, membrane pumps, or adhesion molecules. Antibodies that recognize intracellular components such as histones, lysosomes, signal transducing molecules, and cytokines, to name but a few are available. In particular, the detection of protein activation states with antibodies directed against specific phosphoepitopes, has opened up a new area in which flow cytometry can be used to probe cellular function [18,19].

Antibodies recognize and react against small peptide sequences of complex antigenic molecules. Thus, each antigenic protein contains numerous small peptide sequences, termed epitopes, to which monoclonal antibodies may be raised. Antibodies to any epitope of the parent molecule can be used to identify the entire molecule. Initially, this led to a nomenclature dilemma; each laboratory and commercial source had unique designations for their monoclonal antibodies. To facilitate communication, an international workshop established a consensus nomenclature (see historical review of consensus nomenclature in Chapter 11) [20]. Cell surface antigens were assigned a *cluster of differentiation* (CD) number based on their recognition by monoclonal antibodies. All antibodies to the same antigen, regardless of their epitope specificity, were grouped together. Thus, two or more antibodies, each reactive with a different epitope on the same antigen are considered as directed against the same CD. In general, the antigens themselves are identified by a CD number (e.g., CD3 on T cells) and the monoclonal antibodies recognizing them are grouped as *anti-CD number* (e.g., anti-CD3).

At a workshop held in Vienna in 2006, 350 CD clusters were recognized. These are listed and annotated as Tables 11.2 and 11.3 in Chapter 11. It is important to note that few of the CD antigens are truly restricted to a single cellular lineage. With rare exceptions (e.g., CD3 on T cells), lineage assignments cannot be made on the basis of a single CD antigen. Rather, they are determined by the presence and absence of a combination of markers.

6.3 FLUOROCHROMES AND FLUORESCENCE DETECTION

To detect the presence of a cell-bound monoclonal antibody by flow cytometry, the antibody must be coupled either directly or indirectly to a fluorescent dye (fluorochrome). These are the dyes that, when excited by light of a specific wavelength, emit light at a longer wavelength (this is known as the Stokes shift). Because different dyes have different Stokes shifts, they can be distinguished by passing emitted light through a series of optical filters that permit only specific bandwidths of light to reach the photomultiplier tubes (PMTs) (Figure 6.1). The PMTs generate a signal proportional to the intensity of the incident light. Through spectral compensation, which will be discussed in detail later, the processed signals can be quantitatively related to the amount of dye bound to a particular cell. With appropriate standards, this in turn, can be used to estimate the number of molecules targeted by the fluorescence-tagged antibody.

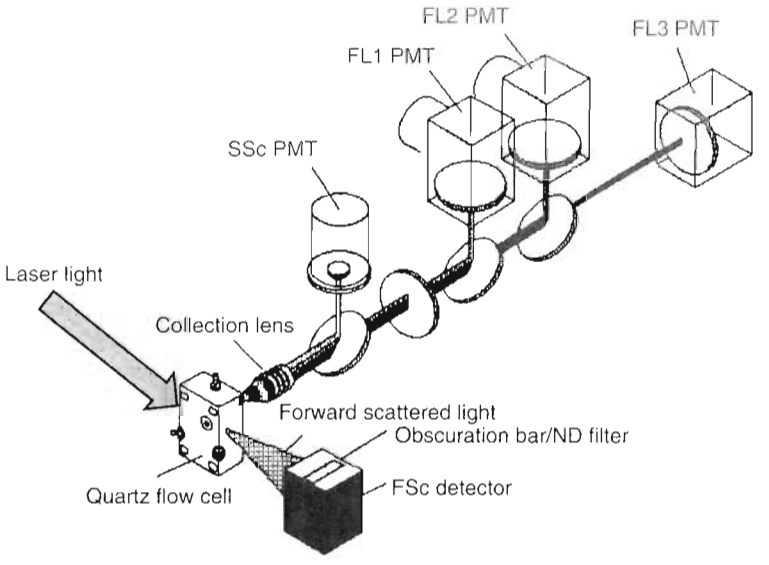

FIGURE 6.1 Schematic operation of a three-color single-laser flow cytometer. The fluorochrome-labeled cells are pumped through the flow cell, where they enter the light path of a 488-nm argon laser (arrow). A photodiode aligned with the laser path captures light scattered between 1.5° and 19° (FSc). Before encountering this FSc detector, the scattered laser light can be attenuated by a neutral density (ND) filter if needed; the laser beam itself is blocked by an obscuration bar. A collection lens is positioned 90° from the incident laser light. This light (which consists of both laser light scattered by the cell and light emitted by the fluorochromes associated with the cell) passes through a series of dichroic mirrors and filters that separates the light sources on the basis of their wavelengths. In the instrument depicted here, light from the argon laser (488 nm) is deflected to the side scatter photomultiplier tube (SSc PMT) by a 488 dichroic long-pass (DL) mirror. Before reaching the SSc PMT, this light passes through a 488-nm band-pass (BP) filter, which blocks all other wavelengths. The use of these filters ensures that the SSc PMT measures only light emitted by the argon laser and scattered at 90° by the cell. The light transmitted through the 488 DL mirror then passes through blocking filters that attenuate any remaining scattered laser light, leaving only the light emitted by the cell-bound fluorochromes. This emitted light is then deflected to the FL1 PMT, using 550-nm DL and 525-nm BP filters. Thus, the FL1 PMT captures a narrow bandwidth of light centering on 525 nm (green fluorescence emitted, e.g., by the dye FITC). In the three-color instrument shown here, this process is repeated two more times, with the FL2 and FL3 PMTs capturing light of progressively longer wavelengths, emitted by additional fluorochromes. Commercially available cytometers with multiple lasers and photodetectors have been used to measure as many as 14 fluorochromes simultaneously, using the same principles (Modified from Beckman Coulter Manual. COULTER EPICS XL/XL-MCL FLOW CYTOMETER, PN 4237340A1-1, 6 April 1998, Elite XL Cytometer.).

In the simplest flow cytometers, light is supplied by a single air-cooled argon or diode laser that emits blue light at a wavelength of 488 nm. Ultraviolet, violet, green, yellow, and red lasers are becoming increasingly common as the list of available fluorochromes grows and multiparameter flow cytometry is more widely adopted. The most commonly used fluorochromes include the old standbys fluorescein

isothiocyanate (FITC), phycoerythrin (PE) and the PE-tandem dyes (PE-Texas red, PE-Cy5, PE-Cy5.5, and PE-Cy7), peridinin chlorophyll protein (PerCP), allophycocyanin (APC), and the APC tandems: APC-Cy5.5 and APC-Cy7. The tandem dyes are of particular importance because they allow a single laser to excite as many as six separate fluorochromes (e.g., FITC, PE, and the PE-tandems can all be excited by a 488-nm laser). PE is a large fluorescent protein that can be excited at 488 nm (but is more efficiently excited by a green or yellow laser), and it emits at 578 nm. It can be decorated with small dye molecules such as Texas red, Cy5, Cy5.5, or Cy7, which are not excited by themselves at 488 nm. Known as *free energy transfer* in physics, the excited PE, instead of emitting a photon at a higher wavelength, directly excites the coupled dye, which then emits light at its characteristic wavelength. Several different PE-tandem dyes with increasingly longer Stokes shifts can be used simultaneously with a single blue or green laser capable of exciting PE. The cyanine and Alexa dye families represent a new generation of *designer dyes*, which are specifically engineered for their excitation and emission characteristics.

Increasingly, antibodies conjugated to a variety of fluorochromes are commercially available. For the direct staining procedure, a cell suspension is initially incubated with one or more dye-coupled monoclonal antibodies directed against the determinants of interest. In the indirect assay, an unlabeled antibody against one target molecule is used to stain the cells. The presence of this antibody is detected by a second labeled antibody. For example, T cells can be identified in human peripheral blood by staining with an unlabeled murine antibody directed against CD3. After washing away the unbound antibody, a fluorescence-labeled goat antimouse immunoglobulin antibody can be used to detect the presence of anti-CD3 on the human T cells. Indirect staining can be used in concert with direct staining, provided the indirect staining is performed first, and all free antimouse immunoglobulin-binding sites are blocked (with mouse serum or purified mouse IgG) before adding the directly conjugated murine antibodies. A relatively new development in which small quantities of monoclonal antibody can be labeled with the antigen-specific portion (FAB) of an antiglobulin conjugated to a dye of choice, provides additional flexibility [21]. Finally, antibodies that are directly labeled with biotin can be purchased. Biotin is not fluorescent by itself, but binds to the tetrameric molecule avidin or streptavidin with an unusually high affinity (hence it's name), which in turn can be conjugated to the dye of choice. This provides versatility, since a biotin-conjugated antibody can be used with your choice of avidin-conjugated fluorochromes, and conversely, the same avidin-conjugated fluorochrome can be used with an array of different biotinylated antibodies.

In addition to the fluorochromes used for labeling monoclonal antibodies, a wide variety of dyes with useful biological properties can be used to identify cell populations or measure functions in living cells (Table 6.1).

6.4 HOW THE CYTOMETER WORKS

After cells have been labeled with dye-conjugated antibodies or other fluorescent molecules, they are resuspended at an appropriate concentration and introduced "single file" into the analytical cytometer. The cell sample is injected into a stream of sheath fluid (saline or distilled water), such that the sample stream forms a stable

TABLE 6.1
Some Commonly Used Dyes and Fluorescent Molecules

Dye	Maximal Excitation/ Emission (nm)	Properties
DAPI [22–25]	358/461 nm, bound to DNA	Binds to AT-rich regions of DNA. Viability staining (viable cells exclude dye); Nuclear (DNA) staining in permeabilized cells
7-AAD [26]	546/647	Viability staining (viable cells exclude dye); Nuclear (DNA) staining in permeabilized cells
Acridine orange [27–29]	495/519	Measurement of DNA and (ribonucleic acid) RNA
Aldefluor [30]	505/513	Nonfluorescent molecule (BODIPY-aminoacetaldehyde) that fluoresces when converted to BODIPY-aminoacetate by aldehyde dehydrogenase (active in stem cells)
BODIPY [31,32]	505/513	Labeling drugs for uptake and efflux studies
CFSE [33]	494/514	Labeling cytoplasmic proteins of viable cells (cell tracking and proliferation assays)
Draq5 [34]	647/670 (huge tail allows excitation with 488 line)	Nuclear (DNA) staining of living (nonpermeabilized) cells
Green fluorescent protein (GFP) and its variants [35,36]	395/509	Identification and sorting of transfected cells. Variants provide alternative excitation/ emissions maxima
Hoechst 33342 [23,37,38]	350/461	Nuclear (DNA) staining of living (nonpermeabilized) cells; Measurement of DNA content (cell cycle); Detection of cells with constitutive MDR transporter activity (side population)
Indo-1 [39,40]	330/401, 475	Intracellular calcium concentration (ratiometric)
JC-1 [41,42]	514/529	Mitochondrial membrane potential
Monochlorobimane [43]	394/490	Measurement of intracellular glutathione
Phi Phi Lux [44]	505/530	Quenched fluorescent molecule linked to the caspase-3 substrate amino acid sequence (DEVDGI). Fluoresces when cleaved by caspase-3 (detection of apoptosis)
Propidium iodide (PI) [45–48]	535/617 nm, bound to nucleic acids	Viability staining (viable cells exclude dye); Nuclear (DNA) staining in permeabilized cells
Rhodamine 123 [37,49]	507/529	MDR transporter-mediated dye efflux, mitochondrial mass

Note: DAPI—4,6-diamidinozphenylindole; CFSE—carboxy fluorescein succinimydal ester; 7AAD—7-amino actinomycin-D; BODIPY—DIPYrromethene BOron Difluoride.

core within the sheath stream. Because laminar flow is established between the two streams, sample and sheath fluid do not normally mix, and the cells are concentrated near the center of the sample stream by a process called hydrodynamic focusing. In an analytical cytometer, which does not have the additional task of sorting the cells,

all this takes place within a quartz flow cell in which the cells are illuminated by one or more lasers. Light scattered by the cells is captured at a small angle (forward light scatter [FSc]) and at 90° (side scatter [SSc]) from the incident light as they cross the laser path (Figure 6.1). FSc correlates well with cell size, whereas SSc measures the cell's internal complexity (nuclear convolutions, vacuoles, etc.). Forward scattered light, because of its intensity, is usually detected by a relatively insensitive and inexpensive photodiode, whereas side scattered light, such as light emitted by the fluorochromes with which the cells are labeled, is measured using very sensitive PMTs. In peripheral blood, small cellular debris, lymphocytes, granulocytes, and monocytes can be distinguished on the basis of their intrinsic light-scattering properties alone (Figure 6.2). The photons emitted by fluorescent dyes associated with the cell are detected by PMTs, which with the aid of a series of filters, limit the window of detection to the major emission region of particular fluorochromes (e.g., with FITC, the intensity of green light, between 515 and 535 nm). The analog output from the PMT, a voltage pulse lasting for the duration of time that it takes the cell to transit the laser line, is converted into one or more numbers that quantify the pulse (area, peak, or duration of the pulse). Precisely, how this is accomplished differs from cytometer to cytometer. The digitized data, often corrected for spectral overlap (also called color compensation) are stored in a data file called a *list-mode* file [50]. Conventionally, these are given the extension *.fcs* or *.lmd*. In some cytometers, both compensated and uncompensated data can be stored in the same file. A typical *list-mode* file can be likened to a large data table in which the columns are the parameters (e.g., FSc, SSc, green, orange, and red fluorescence intensity), and each row represents a distinct *event*. In the parlance of flow cytometrists, *events* are signals that may represent cells but can also be debris or other sources of noise. The process of data collection

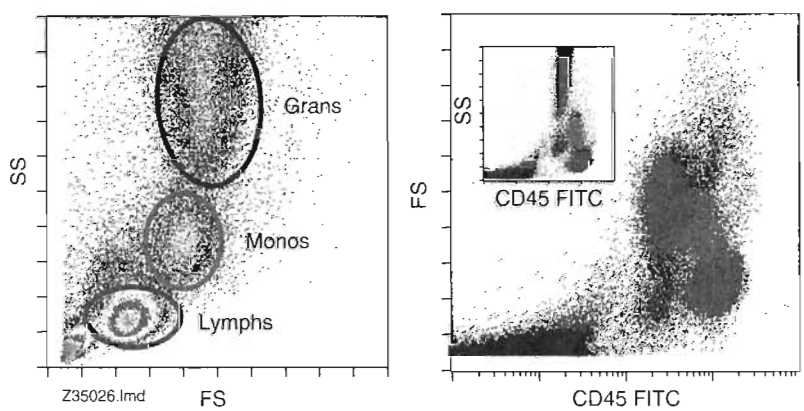

FIGURE 6.2 Discrimination of lymphocyte, monocyte, and granulocyte populations by light scatter. This fixed control cell preparation (CD Chex CD34, Streck Laboratories) was also stained with anti-CD45, a marker expressed to varying degrees on all leukocytes. Color eventing was used to mark the lymphocyte (green), monocyte (red), and granulocyte (blue) populations identified by light scatter alone. Subcellular debris can be seen on the left-hand side of the lymphocyte population. The populations visualized by light scatter also form discrete populations based on CD45 and light scatter (right panel and inset). Note that debris and red cells can be identified by light scatter but are better resolved with anti-CD45.

in which cells are run through the cytometer and parameters describing individual events are stored in data files, is known as *acquisition*. Depending on the complexity of the data, they can either be analyzed in real time during sample acquisition or *offline* by recalling the stored *list-mode* data files.

6.5 SAMPLES

Flow cytometric assays can be performed using anticoagulated blood or bone marrow, isolated cell suspensions, cell cultures, or disaggregated tissue. In peripheral blood, where erythrocytes outnumber white cells by 1000 to 1, it is usually necessary to remove them from the sample. It is not necessary to physically remove platelets and small debris, because these can be *thresholded* out during acquisition (in this case, the cytometer does not count them), *live gated* during acquisition (events are counted but not saved in the list-mode file), or *gated* out on the basis of their low light scatter during analysis. Similarly, cell doublets and clumps can be recognized by their light-scatter properties, and gated from the analysis (Figure 6.3).

As mentioned earlier, normal leukocytes can be segregated into three distinct groups, corresponding to lymphocytes, monocytes, and granulocytes, on the basis of light scatter. A typical three-part differential was illustrated in Figure 6.2. Lymphocytes comprise the leukocyte population with the smallest cell diameter (FSc) and the least internal complexity (SSc). Monocytes are larger cells and have greater internal complexity; neutrophils are cells of approximately the same size as monocytes but

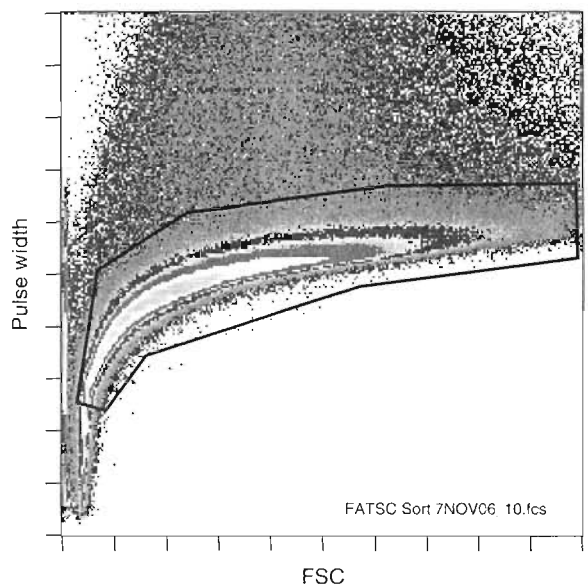

FIGURE 6.3 Doublet discrimination can be performed by comparing pulse analysis parameters. The pulse parameters used for doublet discrimination differ between cytometer manufacturers. The data shown here were collected using a Dako MoFlo sorter, where FSc pulse height (x-axis) is plotted against forward scatter pulse width. Doublets and cell clusters have widths too large for their peaks. Singlets are shown within the polygonal region.

with still greater internal complexity. Because the scatter and fluorescence characteristics of each event are recorded in the *list-mode* file, analysis of collected data can be performed on all events or can be restricted to gated events (i.e., cells that meet predetermined scatter and fluorescence criteria).

Measurement of the percentage of peripheral blood T cells illustrates the principles of flow cytometry analysis. A unique characteristic of mature T cells is the presence of the membrane determinant CD3, a polypeptide that is part of the T-cell antigen receptor complex [51]. At a minimum, T cells can be detected by incubating a cell suspension with a FITC-labeled monoclonal antibody specific for an epitope present on the CD3 determinant. The characteristics of each cell in the suspension are then analyzed and recorded. This includes correlates of two inherent physical characteristics, size (FSc) and internal complexity (SSc), and the intensity of green fluorescence (anti-CD3 FITC) emitted by each cell. Even for a simple three-parameter problem, such as this, there are several ways to approach data analysis. The conventional way is to first establish a *gate* based on forward and side scatter alone to delineate the lymphocyte population. The subsequent analysis of fluorescence is then limited to events with scatter parameters falling within this *lymphocyte gate*. T cells are quantified as a fraction of cells falling within the lymphocyte gate. Although this approach benefits from its simplicity, it does not exploit the fact that T cells and debris are very well separated in the three-parameter space of this assay. Plotting CD3 versus SSc (Figure 6.4) yields a distinct population (raw CD3 gate), which can then be cleaned of early apoptotic T cells or other artifacts by subsequently measuring forward and side scatter on this population. This true T-cell gate then provides guidance for where to make the lower and upper cuts on the lymphocyte gate. The former is often obscured by debris, and the latter by monocytes if we try to draw a lymphocyte gate on ungated events. Once the gates are established, they can be validated against an isotype control and adjusted if necessary. The upper limit of staining with the isotype control can be used to set a fluorescence cutoff; higher fluorescence is considered to indicate specific antibody binding, and therefore the presence of the target antigen. In the present example, the isotype control consists of an FITC-labeled mouse IgG without specific reactivity to human leukocytes and of the same isotype as the anti-CD3 antibody. Although the use of isotype controls is routine in many laboratories, interpretation of the isotype control is subject to several pitfalls. A few of the commonly encountered problems are: control antibodies should be matched with respect to concentration and fluorescence to protein ratio as well as isotype; specific binding can compete with nonspecific binding, such that the negative peak in the control antibody is brighter than the negative peak in the test sample; and positive and negative populations are not always discretely bimodal, but may fuse to form a single skewed distribution that overlaps with the negative control. In this example, CD3+ and negative events are so well separated that an isotope control is not strictly necessary to establish a cutpoint between fluorescence positive and negative cells. In addition to measuring the percent of T cells within the lymphocyte gate, the absolute circulating T-cell count can be calculated by multiplying the percentage of FITC+ cells in the lymphocyte scatter gate by the total number of circulating lymphocytes (cells/μL) determined independently with a hematology analyzer. Inherent in this procedure is the assumption that the flow cytometer and the hematology analyzer detect the same events as lymphocytes.

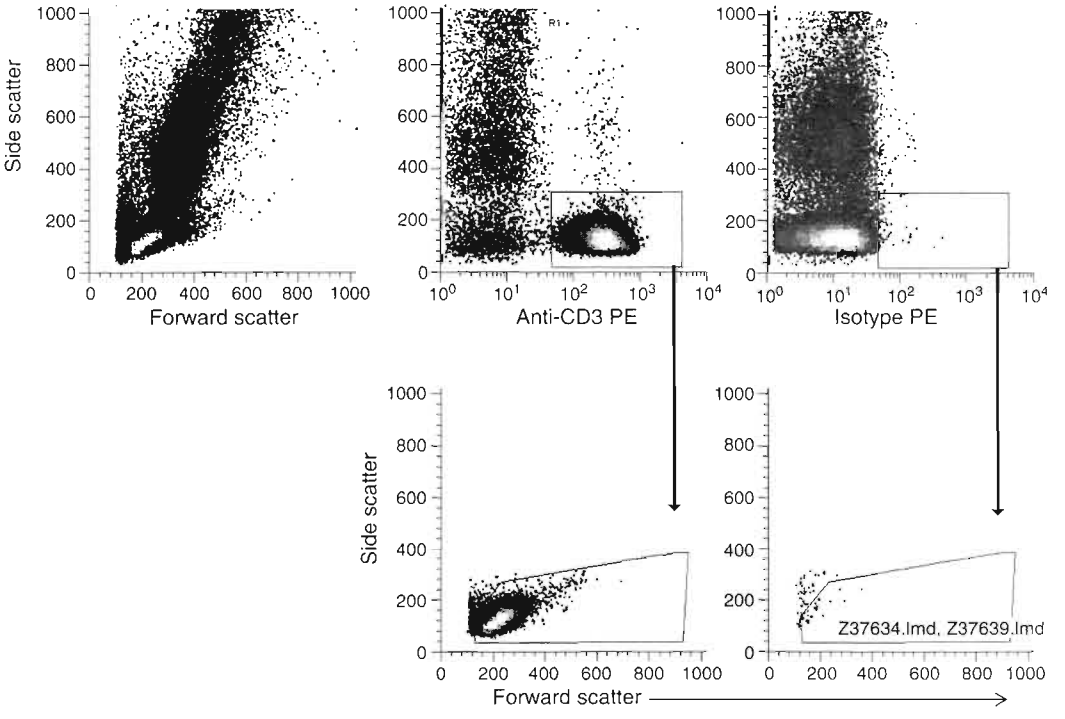

FIGURE 6.4 Gating on CD3 versus SSc prior to creating a lymphocyte gate. Many of us were taught to begin analysis by creating gates on forward and side light scatter. It is our goal to discriminate between cells (the subject of our analysis) and debris, but it is often difficult to see a clear demarcation between these populations on the basis of light scatter alone (top left panel), especially if many events have been acquired. It is often much easier to visualize the population of interest (T cells, in this example) versus SSc. Here (top center panel), a rectangular gate has been created with reference to the isotype control and the expected low SSc characteristic of peripheral T cells. This population can be further cleaned with a conventional "lymphocyte gate" (bottom panels). Note that events nonspecifically binding the isotype control antibody (bottom right) have low FSc and relatively high SSc characteristic of apoptotic lymphocytes.

This assumption is usually correct for fresh blood samples, but not bone marrow or other samples for which the analyzer has not been validated. A more robust *single-platform* method of determining absolute counts by comparison to reference beads is illustrated in Section 6.16.

A major advantage of flow cytometers is their capacity to analyze many different properties simultaneously. The recent invention of the imaging flow cytometer allows a peek at what the cytometer is actually measuring, when cells pass single file before the laser. The principal difference between an imaging flow cytometer (commercially manufactured by Amnis, Seattle, Washington) and a conventional analytical cytometer is that the fluorescent light emitted by the cells, after passing through optical filters, is captured by a sensitive charge-coupled device camera in such a way that separate images of each cell are captured at the wavelength bands corresponding to fluorochrome emissions. As mentioned earlier, a conventional flow cytometer quantifies emitted light using PMTs, and therefore is not capable of assembling this information into images of individual cells. Each individual image captured by an imaging flow cytometer can be analyzed for the intensity of light scatter or fluorescent signals and displayed in much the same way as conventional flow cytometry data are. Additionally, fluorescent signals can be localized to cellular features (plasma membrane, nucleus, cytoplasm, Golgi, lysosomes, etc.). By registering several images of the same cell obtained at different wavelengths, it can be determined whether different fluorescent signals colocalize. This is very important for functional measurements, since signaling molecules often translocate from the cytoplasm to the nucleus when they are activated.

The example given in Figure 6.5 gives a glimpse of what an imaging flow cytometer sees when it looks at a sample of peripheral blood leukocytes stained with anti-CD45 (a pan leukocyte marker), anti-CD14 (a monocyte marker), anti-CD3, and a nuclear dye—Draq5.

6.6 QUALITY CONTROL AND QUALITY ASSESSMENT

If there is a dark side to flow cytometry, it is the perception that artful dial tweaking can make any sample "show whatever the investigator wants." Make a positive sample negative or a negative sample positive? No problem. Even without intentional malfeasance, potential variability in samples, reagents, staining procedures, instrumentation performance and settings, compensation of spectral overlap and data analysis, conspire such that the default condition is often irreproducibility. As the flow cytometry field has matured, so have quality control (QC) and quality assessment procedures. Religious application of these standard measures is a necessary step toward minimizing the most important sources of variation and assuring that the results are interpretable (although not necessarily what the investigator would like). Performance and documentation of QC and assessment measures are routine in clinical laboratories (and are required for certification), but are no less important in research or assay development settings. Rote performance of quality control measures, without understanding their rationale and without knowing how to respond when deviations are detected, may be sufficient to satisfy an inspector, but does

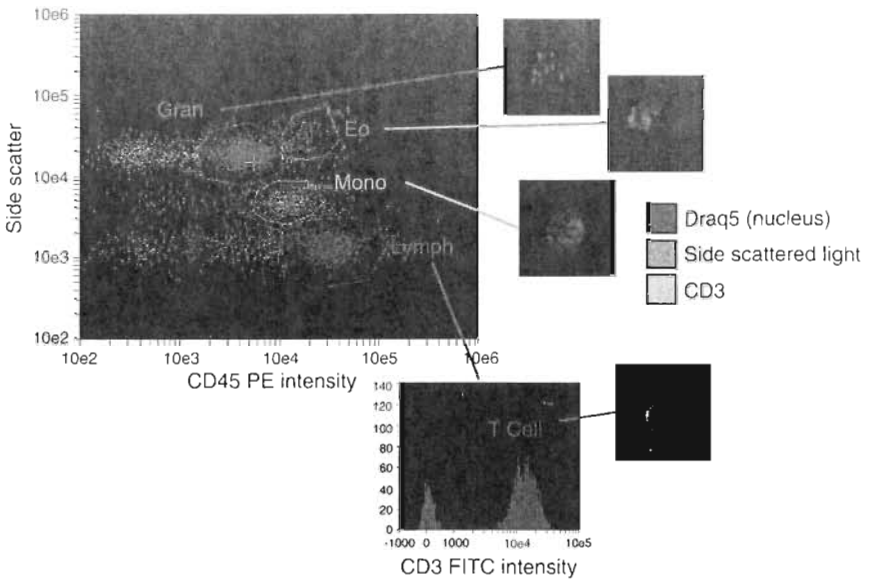

FIGURE 6.5 Imaging flow cytometry provides a glimpse into what a flow cytometer actually "sees" when stained cells are interrogated by a laser, and scattered and emitted light are picked off at 90°. In this example, we chose something familiar: CD45, CD3, and CD14 staining. The DNA intercalating dye Draq5 was used as a nuclear stain. The upper histogram shows patterns of CD45 intensity versus SSc that we would see by conventional flow cytometry. Populations of granulocytes, eosinophils, monocytes, and lymphocytes are identified based on their characteristic patterns. The bottom histogram shows CD3 intensity on cells falling within the lymphocyte gate. All this is very familiar to the flow cytometrist. What is remarkable about imaging flow cytometry is that each event, shown as a dot in the histogram, corresponds to an actual image captured by the cytometer. These images can be recalled simply by clicking on a dot. Alternatively, all the images within a gate can be displayed as a gallery (not shown).

improve assay consistency. This section will consider the most important aspects of quality assessment and control.

QC in flow cytometry includes determining that

- Sample processing is performed correctly
- The instrument is functioning properly
- The instrument settings are consistent
- The regents are behaving as expected
- Data analysis is performed consistently

6.7 SAMPLE ACCESSION AND PROCESSING

As the applications for flow cytometry have grown so have the variety of samples and methods of sample processing. Clinical labs have sample accession criteria, which state the attributes that a sample must have before it is accepted into the laboratory.

For peripheral blood, these may include how the sample is labeled, the elapsed time since sample collection, sample volume, the presence of a particular anticoagulant, and the adequacy of anticoagulation. Failure to meet these criteria results either in sample rejection, or sample acceptance after noting the particular deviation and its probable significance. Prior to performing cytometry, peripheral blood samples are commonly subjected to some form of erythrocyte lysis or removal. Common methods of red cell lysis include a very brief exposure to a hypotonic solution or to formic acid, or a more protracted incubation with ammonium chloride solution. Red cells, mature granulocytes, and platelets may be removed or greatly reduced with a Ficoll–Hypaque density gradient (see details in Section 6.7.2) [52].

6.7.1 Anticoagulation

The common anticoagulants used for peripheral blood and bone marrow samples are heparin, ethylene diamine tetraacetic acid (EDTA), and acid citrate dextrose (ACD). Heparin is a biological product isolated from bovine lung or porcine gut. It is a long negatively charged highly sulfated glycosoaminoglycan that interferes with the clotting cascade by binding to and potentiating antithrombin III. Sodium heparin is nontoxic at a dose effective to prevent clotting (10 Units/mL). It is the preferred anticoagulant when cells are to be used for assays of immune function. Despite its highly charged nature, exposure to sodium heparin does not appear to adversely affect the function of lymphocytes or monocytes. Heparin has an *in vitro* half-life, so it may be exhausted in samples held overnight at room temperature or warmer. EDTA and ACD both work by chelating divalent cations (calcium and magnesium), which are necessary for clotting. EDTA is often the preferred anticoagulant for immunophenotyping samples, whereas ACD is the major anticoagulant used in blood banking and leukapheresis. Neither loses anticoagulating activity with time. Exposure to both agents inhibits calcium and magnesium-dependent cellular processes, so they should be avoided when functional tests are to be performed.

6.7.2 Red Blood Cell Depletion

Ficoll 400 is a sucrose polymer that is perceived as hypotonic by mature granulocytes, but not lymphocytes, monocytes, or immature myeloid cells. Exposure to Ficoll causes granulocytes to dehydrate, which increases their density. Hypaque, a dense radiological contrast medium, is used to adjust the specific gravity of the Ficoll–Hypaque solution to 1.077. Dilute anticoagulated blood is layered carefully on a cushion of Ficoll–Hypaque requiring the same skills needed to make a clean "black and tan" by layering Guinness stout on a cushion of Bass ale. After centrifugation (of the sample, not the drink), the mononuclear cells and platelets are concentrated in a layer at the diluents' Ficoll–Hypaque interface, and the red cells, granulocytes, and dead or dying mononuclear cells form a pellet at the bottom of the tube. The buffy coat is harvested from the gradient interface and washed, removing platelets and residual Ficoll–Hypaque.

After the cells have been processed, cell viability is the major criterion for cell quality. This can be measured independently using Trypan blue dye and a hemocytometer, but it is often convenient to use an exclusion dye directly in the flow assay, provided the cells are not fixed. Appropriate dyes excluded by living cells include

deoxyribonucleic acid (DNA) intercalating agents such as propidium iodide (PI), 7-amino actinomycin D (7-AAD), or 4,6-diamidino2phenylindole (DAPI). The first two are excitable with a blue (488 nm) laser, whereas DAPI requires an ultraviolet (UV) or near-UV violet laser. Because loss of membrane integrity is a late event in the process of cell death, a cell cannot be presumed to be healthy solely on the basis of dye exclusion. However, PI, 7-AAD, or DAPI positive cells have never been known to come back to life. Mario Roederer is fond of saying that you should not try to measure anything on a dead cell. Freshly isolated peripheral blood cells uniformly display excellent viability by dye exclusion, therefore, less than 95% viability may indicate sample mishandling. In contrast, cultured cell samples or single-cell suspensions isolated from disaggregated solid tissue normally contain a significant proportion of dead or dying cells and subcellular debris. These are bad actors in flow cytometric assays, often displaying bright autofluorescent streaks and binding antibodies nonspecifically. Assays on these types of samples often require a viability dye or some other means of identifying and removing these spurious events. If cells are to be fixed after staining, they can be gently permeabilized with saponin and incubated with an intercalating dye shortly before acquisition on the cytometer. Diploid cells with intact DNA will appear as a uniform bright peak, whereas subcellular debris and cells with fragmented DNA will have lower fluorescence (Figure 6.6).

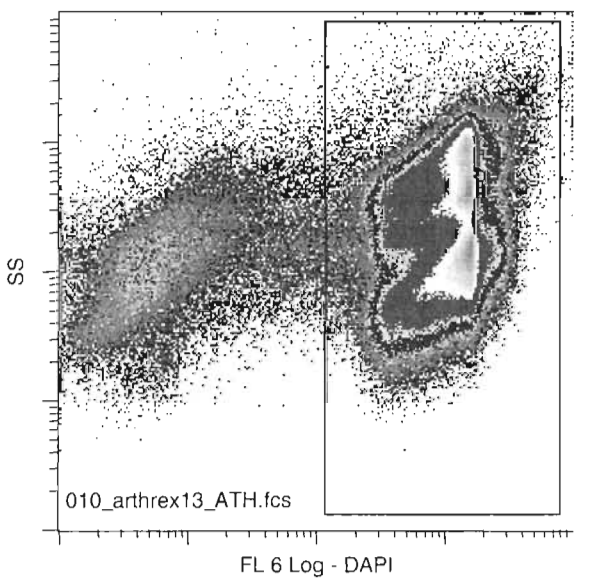

FIGURE 6.6 Eliminating debris with a nuclear stain. This plot represents 2 million Ficoll–Hypaque-separated bone marrow mononuclear cells that were stained, fixed, gently permeabilized, and stained with DAPI. Despite the Ficoll–Hypaque separation, which removes most red cells, mature granulocytes, and platelets, about 6% of the events have less than a complete complement of DNA, indicating that they are red cells, apoptotic cells, or subcellular fragments. Dead cells are often a source of interference in rare event analysis and should be routinely removed by gating.

Cell clumping is sometimes a problem in bone marrow aspirates or single-cell suspension obtained from solid tissue by digestion with collagenase. This clumping is often due to the release of DNA by short-lived granulocytes or other dead cells within the preparation. DNA clumps can be identified by their stringy glistening appearance. DNA slimeballs entrap viable as well as dead cells and should be broken up with DNAase as soon as they are detected.

Cells are often fixed after staining, both to stabilize them and render them non-infectious. Formaldehyde, either freshly prepared from paraformaldehyde, or commercially supplied as methanol-free electron microscopy grade is commonly used at final concentrations ranging from 0.25 to 2%. Most, but not all bound antibodies are unaffected by formaldehyde fixation.

6.8 ASSURING PROPER INSTRUMENT FUNCTION

Flow cytometers are complex pieces of equipment, but the types of failures that result in data corruption are easily identified. The major instrument vendors specify daily QC regimens that differ slightly from one another, but the principles apply to all instruments. The minimum recommended daily QC includes tests of instrument-related variability and validation of PMT settings (voltage and gain). The latter assumes that you already have arrived at settings for each individual fluorochrome (as well as light scatter), and now you want to make certain that a signal of a given intensity gives the same reading (mean fluorescence channel) today as it did yesterday. Although it is desirable to standardize on PMT target channels for a given instrument, the use of very bright or dim fluorochromes or very autofluorescent cells may necessitate assay-specific settings. Arriving at appropriate settings for a given test will be discussed in detail later.

In an improperly functioning instrument, additional variability can be introduced in a variety of ways. Debris in the flow cell can disrupt the laminar flow and hydrodynamic focusing, resulting in turbulence or causing the sample stream to go off center. A misaligned laser or dichroic mirror may decrease sensitivity and add variability. When the sample stream is hydrodynamically focused, the optics are well aligned and the electronics are functioning properly; reference beads manufactured to a very close tolerance limit will show little bead-to-bead variability in the cytometer, as manifested by a very sharp fluorescence intensity peak. A single-bead preparation with broad fluorescence emissions properties such as FlowCheck® (Beckman Coulter) can be used to test all fluorescence parameters and light scatter. Such beads give a single sharp peak in each fluorescence parameter. Typically, signals are acquired with linear amplification, and the mean and standard deviation (SD) of fluorescence intensity are acquired for each fluorescence parameter. The coefficient of variation (CV), computed by dividing the SD by the mean, is determined for each fluorescence parameter and compared to a target CV (typically $\leq$2%). When this test fails, check that the beads are gated in forward and SSc on singlets (beads can clump), clean the instrument with water or bleach followed by water, and try again. The persistence of broad peaks is an indication that service is required. The instrument may still appear to function, but the data will be compromised by the addition of unwanted noise.

Next comes the validation of PMT target channels. For a given cell type and combination of reagents, you will have previously determined target channels for light scatter and fluorescence parameters. Precisely how this is accomplished will be discussed in detail later, but for now assume that you have an assay with which you are satisfied, and you wish to be able to replicate it from day to day. Previously, during assay development you determined the appropriate gain for FSc, and voltages and gains for SSc and fluorescence parameters; you next ran a standard fluorescent bead (e.g., FlowSet™, Beckman Coulter) and determined its geometric mean fluorescence intensity (MFI) in each parameter. These bead intensities were recorded and now comprise the target channels to be hit each time this assay is run. You start with the exact settings (voltages and gains) used last time the assay was run, but adjust these settings for each fluorescence parameter, until the geometric MFI of the standard fluorescent bead is placed exactly in the target channel. The fact that very little adjustment is usually required does not minimize the critical importance of this element of QC. Here, it is important to stress two things: (1) it is the target channel and not the PMT voltage that must be held constant from day to day and (2) if experiments are to be run that require different PMT settings, each experimental setup will have its own set of target channels, which must be validated. In our laboratory, we assign each set of PMT target channels a nickname. When a data file is acquired using these settings, an abbreviation for this nickname is included in the file name. As discussed later, keeping PMT target settings straight is very important when offline compensation is to be used, since the single-stained compensation files must be acquired with the same settings as the experimental data.

The optimal standard bead for validation of PMT settings depends on the instrument configuration. In single-laser systems, a single bead with a broad fluorescence emission spectrum such as FlowSet® may suffice for all fluorescence parameters. In multilaser configurations, you may wish to use beads optimized for each light source. We find that a single-bead preparation (Spherotech Inc., 8-peak Rainbow Calibration Particles®) is sufficiently bright when excited by our violet (405 nm), blue (488 nm), and red (635 nm) lasers. We use the 7th or 8th peak to define our target channels, the lowest detectable peak to validate sensitivity, and all of the peaks to validate linearity.

Sensitivity is a measure of the dimmest signal that an instrument can distinguish from a negative (nonfluorescent) signal. It depends both on the measured difference in fluorescence intensity between dim and negative peaks, and their respective spreads (usually expressed as their CV). Sensitivity can be quantified as mean channel separation of the negative and dimmest peak, which is calculated by taking the difference of fluorescence intensities of the negative and dim peaks divided by a pooled SD of both populations. For a given set of PMT targets, an instrument will have characteristic sensitivities in each fluorescence parameter, which can be validated using multipeak beads (Figure 6.7).

Linearity refers to the relationship between the detected signal and the actual (known) fluorescence intensity over a particular dynamic range. Linearity is assessed using a cocktail of carefully calibrated beads of known fluorescence intensity. The measured fluorescence (geometric MFI) of each peak is plotted versus the reference values provided by the manufacturer and a linear regression analysis is performed (Figure 6.8). The coefficient of correlation (r^2), gives the proportion of

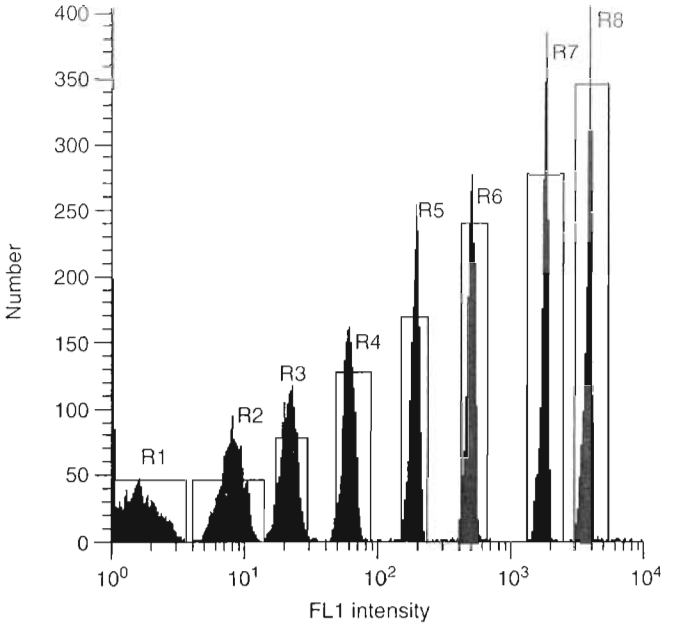

FIGURE 6.7 Use of 8-peak beads to determine sensitivity and linearity. These Spherotech rainbow calibration particles are a mixture of negative beads (R1) and seven bead populations (R2-R7), each containing a known amount of a broadly fluorescent dye (calibrated in equivalents of a given fluorochrome). In the present example, the dimmest peak is easily distinguished from the negative peak, and the brightest peak is on scale.

variation in the measured parameter that is explained by variation in the known values (as reviewed in Chapter 2). A perfect correlation ($r^2 = 1$) means that all of the observed and expected pairs lie along a straight line. A slope of unity means that the measured fluorescence increases in direct proportion to the expected fluorescence. The degree and range of linearity depends chiefly on the instrument design and changes little from day to day. Although it is not necessary to check sensitivity and linearity daily, the data are available if multipeak beads are used for daily validation of PMT settings.

6.9 REAGENT AND PROCESS QUALITY CONTROL

Laboratories that are accredited by the College of American Pathologists (CAP) must satisfy a checklist that includes many aspects of reagent and process quality assessment and control [53]. According to CAP, "The laboratory has the responsibility for ensuring that all reagents, calibrators, and controls, whether purchased or prepared by the laboratory, are appropriately reactive." Further, "verification of reagent performance is required and must be documented." Any of the several methods for reagent validation may be appropriate, such as direct analysis with reference materials, parallel testing of old versus new reagents (known as overlap testing), and comparison with routine controls. When individually packaged reagents or kits are

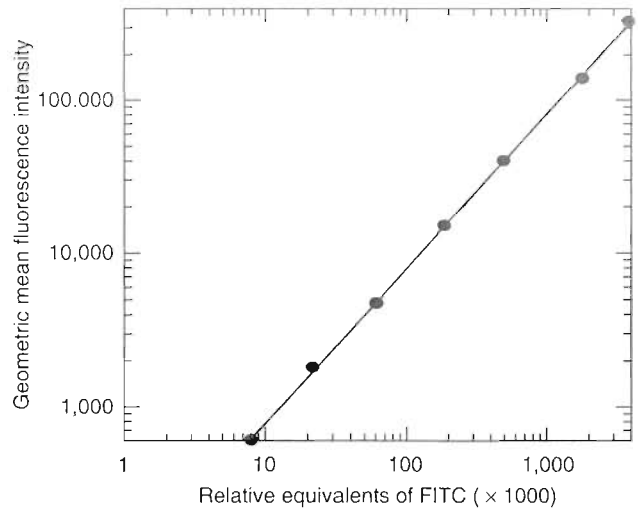

FIGURE 6.8 The use of multipeak beads to determine linearity. The data shown here are the geometric mean fluorescent intensities of the peaks shown in Figure 6.7 (*y*-axis), plotted versus the known FITC equivalents per particle. Note that the unstained peak is not used because 0 is undefined on a log scale. The line shown is the least squares line of best fit of the log-transformed values. The coefficient of correlation (r^2 = 1.000) indicates that virtually all variations in *y*-axis measurements (measured fluorescence) are explained by variations in *x*-axis measurements (fluorescent molecules per particle). The slope of the line is also very close to unity (0.989, standard error = 0.007), indicating a one-to-one relationship between measured and actual fluorescence intensity. We were very pleased to learn that our new cytometer was so linear.

used, criteria must be established to monitor reagent quality and stability. Processing of periodic *wet controls* to validate reagent quality and operator technique is also a typical component of such a system. Records must be kept of each reagent used for each test, its lot number, and the expiration date. Clinical laboratories in the United States that manufacture cellular products for therapy are required by the Food and Drug Administration to follow current Good Tissue Practices (cGTP, as specified by 21 CFR 1270), as well as elements of current Good Manufacturing Practices (cGMP). According to cGMP, newly acquired reagents must be stored separately (quarantined) from reagents currently in use until they have been overlap tested.

In research laboratories, where reagent management is more relaxed and conservation of expensive materials is a priority, it is very important to understand which reagents are stable and which require special care. Monoclonal antibodies themselves have exceptional long-term stability when stored in a sterile environment at 4°C in the presence of a carrier protein such as bovine serum albumin. This is how they are usually supplied, and may also include sodium azide to inhibit microbiological overgrowth. Antibodies conjugated directly with single dyes such as FITC, PE, and APC can also be used for years beyond their nominal expiration dates, providing that they are well protected from exposure to light. In contrast, the tandem dyes, particularly PE-Cy7 and APC-Cy7, pose a QC challenge to clinical and research laboratories alike. Tandem dyes rely on energy transfer from the donor dye (e.g., PE) to the

acceptor dye (e.g., Cy7). When all are working properly, virtually all of the energy emitted by the donor is captured by the acceptor, and there is little or no emission at the wavelength of the donor. However, photobleaching of the acceptor results not only in a decreased intensity at the wavelength of the acceptor, but also in significant emission at the wavelength of the donor. A vial of PE-Cy7-conjugated antibody, if left unprotected in ambient light, will degrade in this manner in a matter of hours. Quality assessment of tandem dye–conjugated antibodies can be incorporated into the daily spectral compensation routine (see Section 6.11).

In our laboratory, we use directly labeled beads (Calibrite Beads, Becton Dickinson) as compensation standards for antibodies conjugated with single dyes (e.g., FITC, PE, and APC). For these dyes, the emission spectrum is a matter of physics, and the emission of a bright FITC-conjugated plastic bead can be used as a standard for any FITC-conjugated antibody. Because the emission spectra of tandem dyes is not identical between antibody preparations, and can change with time for a given conjugated antibody, we run separate single stained controls for each tandem dye–conjugated antibody used on a given day. When the epitope detected by the antibody is both prevalent and bright, readily available cells, such as peripheral blood mononuclear cells from a healthy donor are often used for single-stained controls. We find that the routine use of antimouse Ig capture beads (BD CompBead®, Becton Dickinson) provides a far more reliable compensation standard. These beads are stained with tandem dye–conjugated antibody as one would stain cells, but binding occurs because the antimurine Ig antibodies on the bead's surface recognize a constant region on the murine monoclonal antibody. The result is that virtually any murine antibody (even those that recognize epitopes expressed at low density on rare cell populations) stains the beads with a sharp and bright peak.

The health of a tandem dye can be gauged by examining the fluorescence intensity at the acceptor wavelength, or the amount of compensation needed to correct the *spillover* from the acceptor to the donor wavelength. For example, capture beads single-stained with a bad PE-Cy7 conjugate will have significant spillover into the PE channel. It is important to remember when working with tandem dyes that the stained sample must also be protected from ambient light (e.g., with aluminum foil) and acquired as soon as possible after staining.

The advent of commercial cellular control reagents consisting of gently fixed or lyophilized human cells with published reference values has greatly facilitated process assessment for flow cytometry. These control samples are stained in parallel with test samples. Because acceptable ranges (percent positive and absolute number) are published by the manufacturer, the assay provides an overall metric for quality assessment of the instrument, reagents, staining, and data analysis procedures. An example using CD-Chex Plus® (Streck Laboratories) as a control for a T-cell absolute count assay is shown in Figure 6.9.

Summarizing the total quality assessment process:

- Determine the CV of a homogeneous test bead in each channel. Make certain that the target CV is not exceeded
- Adjust PMT voltage and gain such that standard beads are placed in their target channel

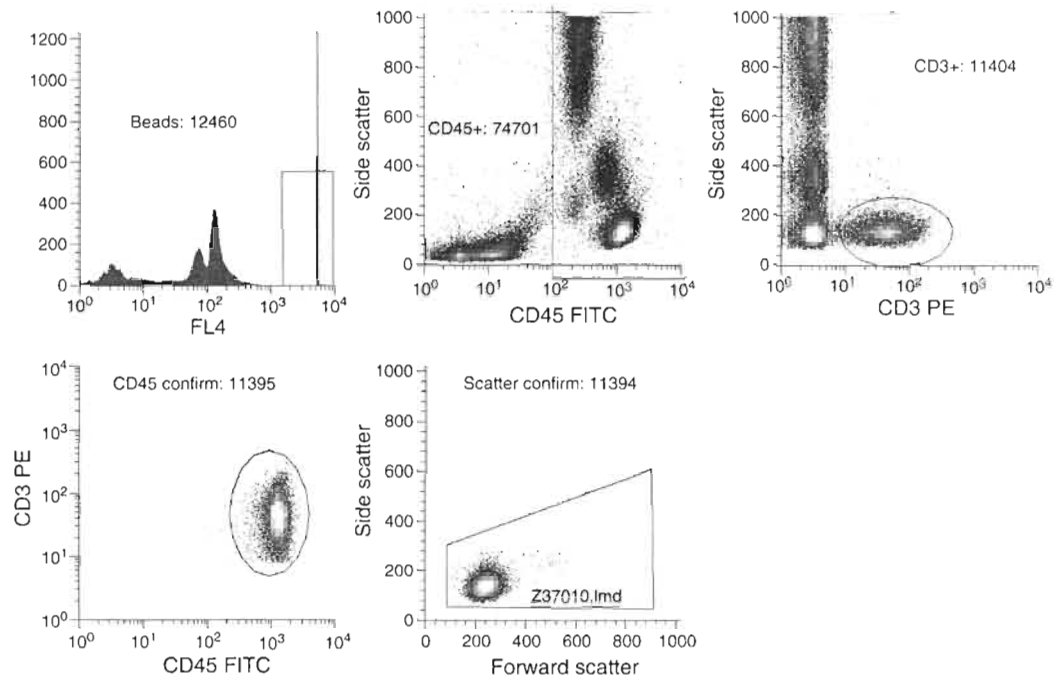

FIGURE 6.9 CD Chex Plus reference standards for the single-platform determination of CD3 absolute count. CD Chex Plus reference cells were stained with anti-CD45 and anti-CD3 monoclonal antibodies and processed according to a *lyse, no wash* protocol. Calibration beads (StemCount, Beckman Coul... ...re detected as a sharp bright peak (*top left*) and the number of events within the peak was determined (12,460). Beads were removed from subsequent plots with a *not* gate. Next CD45+ cells (leukocytes) were identified (*top center*). CD3+ cells with low SSc were identified within the CD45+ population (*top right*) and this population was cleaned up on the basis of CD45 expression (*bottom left*) and light scatter (*bottom right*). The absolute leukocyte count was calculated as the number of CD45+ events (74,701) divided by the number of bead events (12,460), multiplied by the known concentration of the beads (1,022 beads/μL). The T-cell count was calculated similarly. In this example, the measured leukocyte count was 6,127 cells/μL and the measured T-cell count was 935 cells/μL. These values were within the published reference ranges (6,100 ± 500 for leukocytes and 1,179 ± 264 for T cells).

- Determine linearity and sensitivity of the instrument in each channel using multipeak beads
- Stain Ig capture beads with all tandem dye–conjugated reagents to be used for the day
- Determine and evaluate PE spillover for all antibodies conjugated to tandem dyes by staining Ig capture beads
- Create compensation matrices using Ig capture beads for all tandem dye antibodies and integrally stained beads in place of all single-dye conjugated antibodies
- Stain a verify tube using control cells (e.g., CD-Chex Plus®) (acquire data and compare observed and expected values)
- Graph and monitor PMT voltages required to meet target channels as a function of time (Levey-Jennings plots, see Section 6.14)

6.10 CHOOSING PHOTOMULTIPLIER TUBE GAIN SETTINGS

In the early days of flow cytometry, choosing proper PMT settings was a simple task. Unstained cells, usually human peripheral blood mononuclear cells, were run and the PMT voltage and gain settings were adjusted until the peak of this negative sample was placed within the lower portion of the first decade of log fluorescence intensity plots. Care was taken not to let more than half of the cells fall *off axis* (i.e., in the first channel). This process was repeated for each fluorescence parameter. Two things have changed that make this process a bit more challenging. First, the use of multiple laser lines and far red and infrared emitting dyes means that the intrinsic fluorescence (autofluorescence) of unstained cells is not equivalent across the fluorescence parameters. Second, in the days of entirely analog signal processing, a good part of the signal detected in the first decade was due to instrument noise, and thus independent of sample. Modern cytometers are still imperfect at the lower end of the first decade, but improved signal processing requires one to define where in first decade artifact ends and the signal begins. For newer instrumentation with digital signal processing, Holden Maecker of BD Bioscience recommends plotting the CV of an unstained sample as a function of PMT voltage, gradually moving the peak across the first decade. As the voltage is increased, the CV decreases sharply initially and then levels off (Figure 6.10). This is due both to raising a greater proportion of events off axis (increasing the mean and therefore lowering the CV) and to an actual sharpening of the peak as the contribution of instrument noise diminishes. After the voltage setting at which the CV levels off has been determined, standard beads are run at that setting to establish the target bead channel (channel in which the bead peak falls). This target channel must be reproduced during daily QC. Beyond this, there are two more factors to be considered in selecting PMT target channels: (1) The brightest positive signals to be encountered in stained samples must be on scale (data in the last channel cannot be compensated for spectral overlap) and (2) The PMT settings for the different fluorescence parameters should be sufficiently balanced to permit compensation for spectral overlap. Why this is important will be explained in Section 6.11.

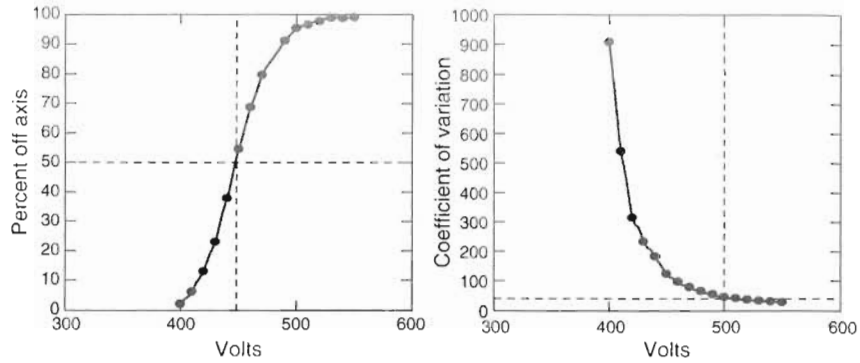

FIGURE 6.10 Determination of the optimal PMT voltage on unstained peripheral blood lymphocytes. Unstained peripheral blood cells were acquired within a lymphocyte light scatter gate. For each fluorescence parameter, the PMT voltage was gradually increased and the percent of events falling on scale and the CV of the peak were determined at each voltage setting. The results were plotted, and negative exponentially weighted curve smoothes were applied to the points. The example shown here is for the FL1 PMT, which was set up to measure green fluorescence. At the lowest voltage tested, most of the cells were off scale (i.e., piled up in the first channel) and the CV was very high. At 450 V, about half of the cells were on scale (left panel, dashed lines), but the CV was still relatively high. This would be the lowest recommended setting, and would be used if very bright events were to be acquired in FL1. The CV continued to decrease with increasing voltage and was close to its lower asymptote at 500 V (right panel, dashed lines). This would be the preferred setting for the majority of cases. It is important to note that this setting is optimized for peripheral blood lymphocytes, which have relatively little autofluorescence. Different settings may be required for cultured cells or disaggregated solid tissues.

6.11 COLOR COMPENSATION MADE SIMPLE

Spectral or color compensation has been treated extensively elsewhere [54–57]. Yet, it remains the most common source of error and vexation for cytometrists everywhere. This section is meant to be a practical guide to understanding and avoiding the pitfalls of color compensation, rather than a complete exploration of the physical principles and mathematics. Color compensation can be thought of as correcting for the spillover of a given fluorochrome from the fluorescence channel in which it is intended to be measured to all of the other fluorescence channels. The spillover coefficient from channel A into channel B ($SC_{A\rightarrow B}$) (e.g., from the FITC channel into the PE channel) is measured by running a single-stained sample meant to be detected in channel A and dividing the geometric MFI of the peak detected in channel B (FI_B) by that of channel A (MFI_A) (Figure 6.11):

$$(SC_{A\rightarrow B}) = \frac{MFI_B}{MFI_A}$$

This spillover coefficient, $SC_{A\rightarrow B}$, gives the proportion of the signal detected in channel A that will be spuriously detected in channel B. It is dependent not only on the emission spectrum of the particular fluorochrome, but also on the relative gains

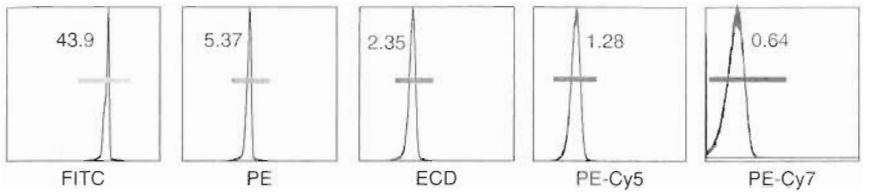

FIGURE 6.11 Determining spillover coefficients. FITC-labeled Calibrite beads were acquired and the geometric MFI was determined for each fluorescence parameter. The *x*-axes are labeled corresponding to the fluorochromes to be measured in the experimental setup. The spillover of FITC into the PE channel can be expressed as the MFI of FITC beads in the PE channel divided by the MFI of FITC beads in the FITC channel. In this example, it is 12.2%. The greater the difference in emission wavelength between FITC and the other fluorochromes, the lower the spillover. This is not the case for tandem dyes, which often have significant spillover at the emission wavelength of the donor dye.

of the two PMTs. Spillover coefficients can also be conceived of and calculated as slopes, since $SC_{A\rightarrow B}$ is the change in MFI_B as a function of MFI_A.

In a two-color instrument, where spillover and compensation coefficients are almost identical, the fluorescence intensity of an event detected in channel B can be corrected for spectral overlap (FI_{BComp}) by subtracting the fluorescence intensity detected in channel A multiplied by the spillover coefficient of A into B:

$$FI_{BComp} = FI_B - (FI_A \times SC_{A\rightarrow B})$$

The two-way spillover coefficients (A into B and B into A) are minimized, and thus compensation is minimized, when both PMTs are balanced. PMT balance cannot be achieved by applying equal voltages to the two PMTs, because PMT sensitivity is not standardized and often very different voltages are required to achieve equal results from different PMTs. Further, perfectly balanced PMTs are not always desirable. If you wish to detect a dim signal in channel B, the gain of PMT_B can be increased relative to that of A. This will result in greater spillover of A into B (and hence greater compensation) and less spillover of B into A (less compensation). This may seem counterintuitive, but consider how we defined the spillover coefficient. Similarly, it may be necessary to lower the sensitivity of a PMT if it is used to detect an exceptionally bright fluorochrome. It is for these reasons that PMT target channels cannot be chosen solely by evaluation of unstained controls, and it is often necessary to have different PMT target channel sets for different applications.

One more item remains to be addressed before we leave the theoretical, and that is the difference between spillover and compensation coefficients. As we mentioned earlier, they are very close, but not identical in a two-color problem. As the number of fluorescence parameters increases they further diverge. For example, when three fluorochromes are used, the total signal detected in channel A results from the true signal from fluorochrome A, plus the spillover of fluorochrome B into A, plus the spillover of C into A. We wish to correct (compensate), such that the effects of spillover are eliminated and only the true signal from fluorochrome A is measured. But the proportion of the signal in B to be subtracted from A is not correctly described by the spillover

coefficient of B into A, because some of the signal detected in channel B is due to spillover of A into B and C into B. Fortunately, this type of a problem is addressed by the field of linear algebra and the true compensation coefficients can be described by a series of simultaneous equations and solved with matrix algebra. All modern automated compensation software use this algorithm, sometimes referred to as the *matrix inversion* method [58].

Now that we have seen why color compensation is necessary, we can examine practical ways in which it can be implemented and assessed in simple and complex applications. The CD34 test used in our clinical laboratory (StemKit™, Beckman Coulter) is nominally a four-color assay, but one fluorescence channel is used to identify viable cells by 7-AAD exclusion, and one channel is used to detect StemCount® beads as a reference for absolute cell counting. Thus, we have a two-color compensation problem (anti-CD45 FITC versus anti-CD34 PE). Because these are single dyes for which the emission spectra are constant, the amount of color compensation required should never change, provided the PMT gains are consistent from day to day (this is ensured by validating the PMT target channels). However, accrediting bodies such as the CAP require color compensation to be validated on a regular basis. For the CD34 assay, we validate our compensation settings weekly using unstained, FITC and PE Calibrite® beads. We use the same fluorescence PMT settings to be used in our assay (but different forward and side scatter, adjusted for bead detection). These settings are adjusted daily against FlowSet™ beads. In the clinical laboratory, we are still using a very *mature* software package (System II®, Beckman Coulter) that includes a semiautomated compensation algorithm, which mimics old-fashioned manual compensation by matching the fluorescence intensity of the negative population with that of the stained beads (e.g., compensation is increased until the intensity of the FITC standard in the PE channel matches that of the unstained beads). We have not found it necessary to change the compensation values over a period of years, providing an additional independent validation of the PMT settings. Real-time data analysis is performed during data acquisition using the validated compensation values; compensated data are saved to list-mode files containing the original analysis protocol, in case reanalysis is necessary.

For complex multicolor analyses, real-time color compensation and data analysis may not always be feasible or desirable. Further, the classical technique of matching median fluorescence intensities described earlier is not the most efficient or the most accurate. All modern flow cytometry analysis software packages support offline compensation. Compensation is computed from measurements of spillover or slopes of single-stained samples, using the sweet range of the cytometer rather than the troublesome first decade. The advisability of performing a fully automated compensation on multicolor data cannot be over emphasized.

As detailed previously, PMT setting validation, linearity, and sensitivity testing are done daily, and single-stained beads (directly labeled or Ig capture) are acquired for each run. It is critical that the single-stained control beads be acquired at the same fluorescence PMT settings as the actual samples, and for tandem dyes, that the single-stained controls be performed with the actual labeled antibodies used to stain the sample.

Compensation matrices derived from mix-and-match single-stained bead list-mode files are computed and applied during data analysis. When tandem dyes are

used, it is not unusual to create four separate compensation matrices for a panel consisting of four tubes. Data-presentation aids that allow on-axis events to be visualized (e.g., Baseline Offset from Beckman Coulter and Log Bias from Verity Software House) must never be used during compensation, because even grossly overcompensated events appear to be perfectly compensated.

With the exception of DNA, ploidy measurements, and a few other specific applications, most fluorescence data are conventionally displayed on a logarithmic scale. Compared to a linear scale, a log scale emphasizes (spreads out) lower values and compresses higher ones. It also normalizes the distribution of fluorescence intensity within a given cell population, and is a very useful way of visualizing data that is distributed over a wide dynamic range. Zero and negative numbers are undefined on a log scale, and this often creates a problem causing data to *pile up* on the axes. A new family of data display scales (biexponential, hyperbolic sine function, HyperLog [59]) offers the best of linear and log displays. These scales are approximately linear on the low end of the scale and become logarithmic at higher values. Like a linear scale, 0 and negative values are defined. This is very useful for evaluating compensation, since the mean Fl_{BComp} for a sample single-stained with A should be 0. Because measurements have variance (spread), a symmetrical distribution of the data around the mean of 0 means that there will be both positive and negative values. This is easily visualized in a HyperLog plot (Figure 6.12), but missed entirely in a conventional log display where 0 and negative values are undefined, and events with fluorescence less than or equal to the lowest value defined in the scale are crowded together on the axis. It will take time before this type of display is universally accepted and it is not without problems (determining how much graphic space to devote to negative values

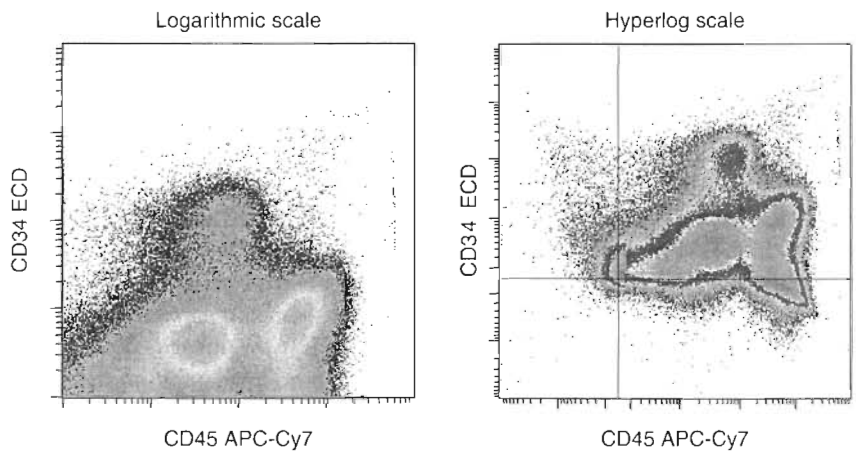

FIGURE 6.12 Use of the HyperLog scale to evaluate spectral compensation. In this example, the same data are displayed on a conventional logarithmic scale (left panel) and on a HyperLog scale (right panel). The origin of the quadrants on the right panel indicates fluorescence intensities of zero. Zero and negative values are undefined on the logarithmic scale, and all such values pile up on the axes. When data are properly compensated, negative populations are symmetrically distributed about the origin.

is difficult because the range of negative values can be quite variable). However, it solves far more problems than it creates, and is likely to become the standard.

One more word on compensation standards: When using tandem dyes we strongly recommend against using cells stained with a bright antibody (e.g., CD45 PE-Cy7, CD8 APC-Cy7) as a compensation standard for other antibodies conjugated with the same tandem dye. Although this is recommended by some cytometer manufacturers, it makes the assumption that both antibodies require the same amount of compensation. This is asking for trouble.

6.12 QUALITY CONTROL FOR ABSOLUTE COUNTS

The single-platform absolute count method using the *lyse no wash* method is widely used for determining absolute CD34 or T-cell counts (i.e., quantifying the concentration in cells/microliters). The principle is simple. According to one popular method, a known and carefully measured volume of sample is deposited in a tube and stained by the addition of directly labeled monoclonal antibodies. After staining, the red blood cells are lysed by the addition of a large excess of ammonium chloride–based lysing solution. Calibration beads of known concentration, of volume equal to the sample volume and measured with equal care, is then added. After gentle mixing, a viability dye is added and the sample is acquired on the flow cytometer. Because the sample was never washed, there is no opportunity for cell loss. It is of little consequence that the unbound antibody is still present in the sample; pulses caused when labeled cells are interrogated by the laser are measured relative to the background fluorescence of the sample stream (baseline) and thus are seen above the noise caused by unbound fluorochrome. During analysis, the internal standard beads are identified by their unique scatter and fluorescence profile. The number of bead events is counted and compared to the number of events of interest (e.g., CD45+ CD34+ cells). The absolute count is determined as the number of events of interest divided by the number of beads and multiplied by the known bead concentration. Given proper instrument performance and accurate gating of the beads and the events of interest, there are only two key steps in the process: The beads must be handled properly (brought to temperature and gently mixed) to assure that the bead concentration added is the same as that stated by the manufacturer (usually about 1×10^6/mL). The same pipetting device should be used for beads and sample, because the precision of volume measurement is critical (see Chapter 2, Statistics, for a discussion of precision versus accuracy). A positive displacement pipette is best for this purpose. Note that the volumes of antibody and lysing solution do not enter into the absolute count equation and are therefore not critical. Beyond relying on the bead concentration stated by the manufacturer, bead concentration can be independently confirmed on a hematology counter. An example of the single-platform method is given in Section 6.16.

6.13 QUALITY CONTROL FOR QUANTITATIVE FLUORESCENCE

Flow cytometers are so linear and perform well over such a large dynamic range that it is natural that they should be used for making quantitative measurements of proteins and other molecules detected on single cells. The problem has always been one

of calibration. How many molecules do you have on a cell when they have a particular MFI? The fluorescence of CD4+ T-cells can be used as a *poor man's* quantitative standard, providing that (1) normal peripheral blood mononuclear cells, which are known to express on average 50,000 CD4 molecules per T-cell [60], are used as the standard; (2) antibody conjugation is well controlled, such that antibodies being compared have identical fluorescence to protein ratios (PE is easiest, since a well-conjugated antibody has one PE molecule per antibody molecule); and (3) the antibodies are used at epitope saturating concentrations. The number of molecules of interest can then be calculated by taking the ratio of the geometric MFI of the molecule of interest divided by that of the CD4+ population and multiplying by 50,000 [61]. A more elegant and better-accepted method involves the use of a series of multipeak beads calibrated in terms of molecules of equivalent soluble fluorescence (MESF) units (Quantum Beads®, Bangs Laboratories). The beads are run daily and a linear regression is performed on geometric MFI of the beads versus known MESF. The MESF of the experimental sample is then determined by plugging the MFI of the unknown into the regression equation. The measurement of ZAP 70 expression in chronic lymphocytic leukemia provides a clinical example of the utility of quantitative fluorescence as a prognostic indicator. An excellent paper by Chen et al. [62] compares several methodologies, including quantitative fluorescence determined as molecules of equivalent soluble fluorochrome, in the context of ZAP 70 measurement.

6.14 USE OF LEVEY–JENNINGS PLOTS

Levey–Jennings plots provide a handy way to examine QC data for trends over time and a suitable means for the periodic review of QC data (Figure 6.13). Levey–Jennings plots can be used to show results (percent positive of a process control standard) or settings (such as the voltage required to hit a PMT target channel) as a function of time. Rather than show raw results on the *y*-axis, Levey–Jennings plots transform the data by subtracting the mean of a series of historical observations, and then scaling the results in terms of SDs (calculated from the same historical values). This transformation provides an enormous advantage over merely plotting the raw data. Assuming that normally occurring random fluctuations in performance have a Gaussian distribution,

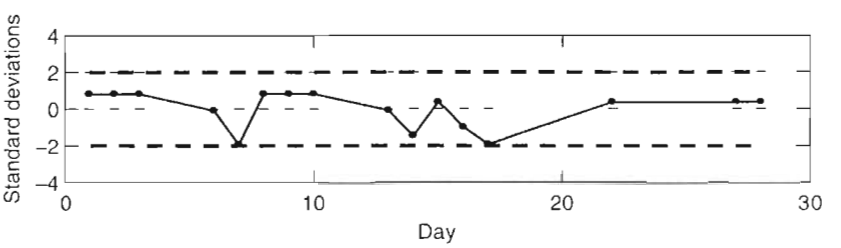

FIGURE 6.13 Levey–Jennings plot of changes in FL1 voltage with time. The *y*-axis is scaled in SD units. Dashed lines show a range 2 SD below and above the mean. Over the plotted time period, the average voltage required to meet the target channel, as defined with FlowSet beads, was 760 V ± 2.2 (SD). Here, the SD (2.2 V) is so small that we are not concerned that the voltage dropped almost 2 SD below the mean on days 7 and 17.

the Levey–Jennings scale facilitates a probabilistic interpretation of daily QC results. All positive data are above the mean historical value, and all negative data are below it. A value one SD above or below the mean has a 32% probability of occurring as a result of random fluctuation. Results 2 and 3 SDs beyond the mean would be expected only 4.6 and 0.3% of the time, respectively. When it is improbable that a fluctuation of a given magnitude has occurred by chance, it implies that something has changed that has caused your results to fall outside your historical norms. Even for samples falling well within the expected range, the probability that two consecutive values fall above the mean (0 on the Levey–Jennings plot) is high (1 in 2), but the probability of six consecutive values lying above the mean is only 1 in 32, and therefore indicative of drift.

6.15 DON'T QC LIKE A MONKEY

We know of laboratories in which QC is performed religiously but seldom if ever acted on, and laboratories in which thorough QC is performed for a standard setting, but not the predominant settings currently used by the laboratory. Regrettably, such missteps have even cropped up from time to time in laboratories under the author's direction. The key is understanding deeply that QC is not *just* a thankless chore (which it undoubtedly is); but, additionally, it is the only thing that separates the reproducible from the irreproducible. How to avoid QC'ing like a monkey? Look at the results with a practiced eye:

- Are the CVs of your standard beads getting wider?
- Has there been a sudden increase or an increasing trend in the PMT voltages needed to meet your target channels (the Levey–Jennings plot is a great way to spot this)?
- Has the dimmest peak that you can resolve with multipeak beads changed?
- Is the PE or APC spillover of individual tandem dye conjugated antibodies increasing?
- Do you have to make unexplained adjustments in scatter or fluorescence analytical regions?

Such changes may indicate an instrumentation problem, such as a failing component, misalignment, a vacuum leak, or a dirty flow cell, any of which could compromise data integrity.

6.16 TWO PRACTICAL EXAMPLES

This section provides two practical examples of assays used in the clinic that came directly out of the research laboratory. The first provides a means of measuring absolute T-cell counts in samples where the frequency of T cells is low. We use this test in the hematopoietic stem cell laboratory to quantify T cells in T-depleted stem cell graft products. It provides an example of a bead-calibrated single-platform assay, and provides an opportunity to review the principles of rare event detection. The second

example examines the detection of cutaneous T-cell lymphoma in the blood by T-cell receptor (TCR) v-beta analysis. It provides an example of the classifier/outcome gating strategy recommended for multiparameter flow cytometry problems, as well as a clever use of fluorochromes to measure six specificities using a five-color instrument.

6.16.1 Single-Platform Detection of Absolute T-Cell Counts as Rare Events

Beckman Coulter pioneered the clinical use of the single-platform *lyse no wash* assay when it introduced the StemKit, a test for quantifying CD34+ cells. StemKit is labeled for IVD use in the United States and is also CE-marked (the equivalent in the European Union). Single platform means that absolute counts (cell/μL) can be obtained using only a conventional flow cytometer (in contrast, a dual platform assay would relate CD34 percent in a sample to the white blood cell [WBC] determined on a hematology analyzer to determine CD34+ cells/μL). *Lyse no wash* means that a whole blood sample is stained and erythrocytes are lysed without a wash step. This eliminates the inevitable loss of cells when centrifuging and decanting. We have used the principles of the StemKit assay to develop an in-house test to quantify T cells in samples in which they are very rare, for example, in the blood of patients immediately after myeloablative or immunoablative therapy, or in T-cell depleted graft products. Such *home brew* assays are classified as *analyte specific reagent* (ASR) tests by the Food and Drug Administration (FDA), and can be reported for clinical use providing that the laboratory has proper Clinical Laboratory Improvement Amendments (CLIA) certification, and the report is accompanied by an ASR disclosure. In our CD3 rare event assay, the number of replicates to be run depends on the WBC, with six replicates run when the WBC count is 250 cells/μL or less. In this case, heparinized blood (200 μL) is added to seven tubes very precisely with a positive displacement pipettor. Six tubes are stained with anti-CD45-FITC/anti-CD3-PE and one is stained with anti-CD45-FITC/isotype-PE. After staining, cells are lysed by the addition of 2 mL of ammonium chloride lysing solution. 100 μL of StemCount Fluorospheres® (at a known concentration stated by the manufacturer) are added with the same pipettor used for the sample. After the addition of the viability dye, 7AAD, the cells are held on ice and exhaustively acquired on the flow cytometer. The six replicate stained samples are acquired first. Because the entire volume of each of the 6 samples is acquired, this is the equivalent of counting every cell in 1.2 mL of whole blood. A blank tube is acquired next to minimize sample carryover, followed by the isotype control tube. Figure 6.14 shows typical results for a patient sample assayed 3 days after receiving an immunoablative regimen consisting of cyclophosphamide, fludarabine, and antithymocyte globulin. Figure 6.15 shows data from the same patient immediately after having completed the therapy. The data are shown in reverse chronological order to explain the gating strategy better. Only one of six replicate determinations is shown, but the replicates were used to calculate confidence intervals about the determinations. The patient's T-cell count nadired at 0.84 ± 0.11 CD3/μL at day 0 (mean ± SEM), and had recovered to 7.83 ± 1.40 CD3/μL 3 days later.

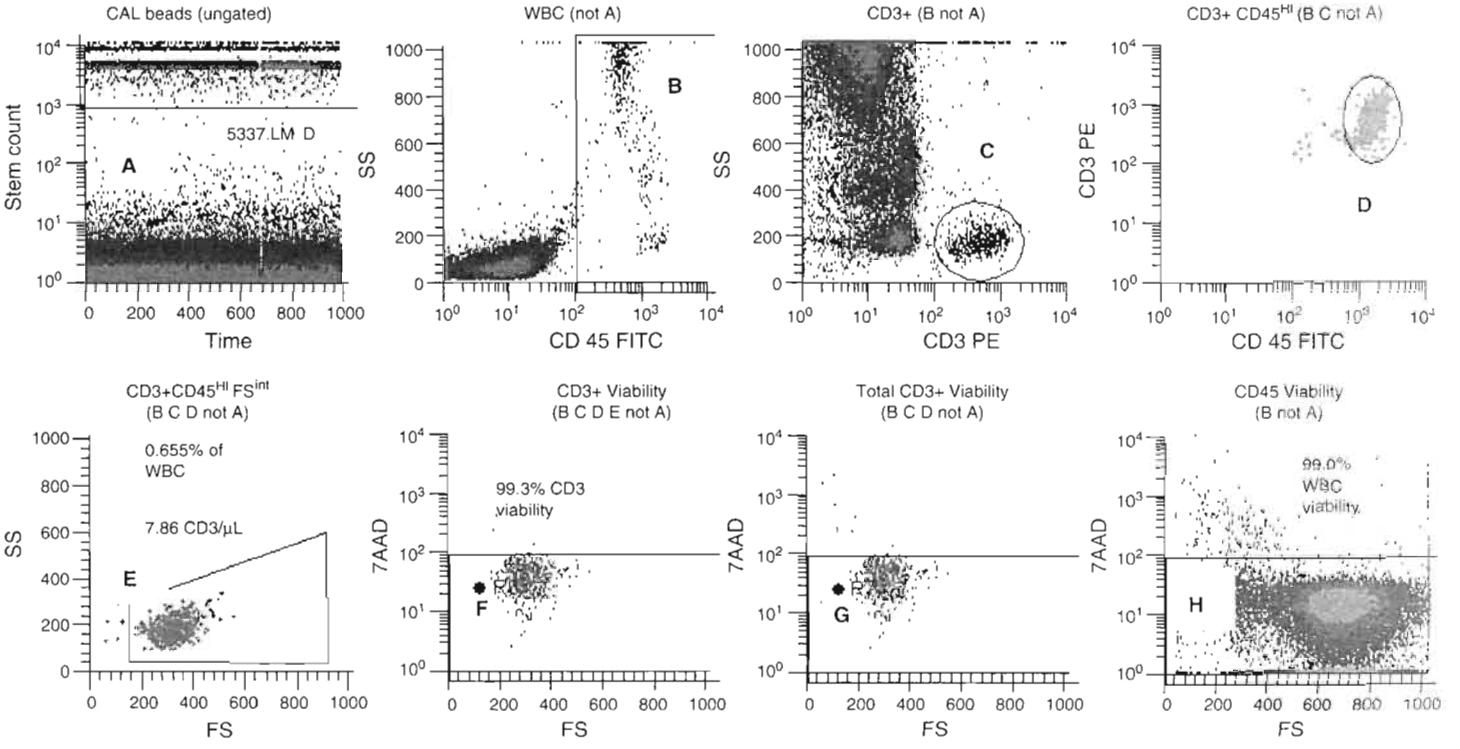
CAL beads (ungated)
Stem count
Time
5337.LM D
A
WBC (not A)
SS
CD 45 FITC
B
CD3+ (B not A)
SS
CD3 PE
C
CD3+ CD45HI (B C not A)
CD3 PE
CD 45 FITC
D
CD3+CD45HI FSint
(B C D not A)
0.655% of
WBC
7.86 CD3/µL
E
SS
FS
CD3+ Viability
(B C D E not A)
99.3% CD3
viability
F
7AAD
FS
Total CD3+ Viability
(B C D not A)
G
7AAD
FS
CD45 Viability
(B not A)
99.0%
WBC
viability
H
7AAD
FS

FIGURE 6.14 Detection of CD3+ T cells as rare events in the peripheral blood of a patient three days after completing immunoablative therapy. To achieve maximum sensitivity, whole heparinized blood (200 μL) was stained with anti-CD45-FITC and anti-CD3-PE in six-plicate and cells were acquired to exhaustion. StemCount beads are identified by their high fluorescence in FL4 versus time (gate A). These are removed from subsequent analyses using a *not gate*. Collecting time as a parameter facilitates identification of fluidic and other instrument problems during sample acquisition. WBCs are identified by CD45 expression (gate B). Note the extraordinary amount of debris. The WBC gate, compounded with the not bead gate is passed to a histogram of anti-CD3 versus SSc. CD3+ events with low SSc are identified (gate C). The compound gate of WBC, not bead, and CD3+ is passed to a histogram of CD45 versus SSc, where T cells are distinguished from noise by their bright expression of CD45 (gate D). No events fitting these criteria were seen in the isotype control (not shown). The compound gate of WBC, not bead, CD3+, and bright CD45 expression is passed to a histogram of forward scatter versus SSc (gate E), which is used to eliminate events with low forward scatter. The number of CD3+ cells obtained in gate E, taken as a percent of WBCs identified in gate B, represents the percent of CD3+ cells. For determination of the viability of CD3+ cells, the compound gate of WBC, not bead, CD3+, bright CD45 expression, and intermediate to high forward scatter is passed to a histogram of forward scatter versus intracellular 7AAD concentration (FL3). Because 7AAD is excluded by viable cells, viable CD3+ cells are detected in region F. Even in samples with low overall viability, the proportion of dead cells within the F region is invariably low. This is because the majority of dead and dying cells have low forward scatter and are eliminated by gate E. It is for this reason that we measure and report CD3 viability using a compound gate of WBC, not bead, CD3+, and bright CD45 expression, where viable CD3+ cells are detected in region G and reported as a percent of cells in gate D. Similarly, viable WBCs are detected in region H and reported as a percent of cells in gate B. Absolute WBC and CD3 counts are obtained by dividing the events in gates B and E, respectively, by 2 (the ratio of sample volume to bead volume); dividing by the number of beads in gate A; and then multiplying by the known StemCount bead concentration (1×10^6/mL). In this sample, CD3+ cells represented 0.655% of CD45+ events. The viability of total WBCs (CD45+) and CD3+ cells exceeded 99%.

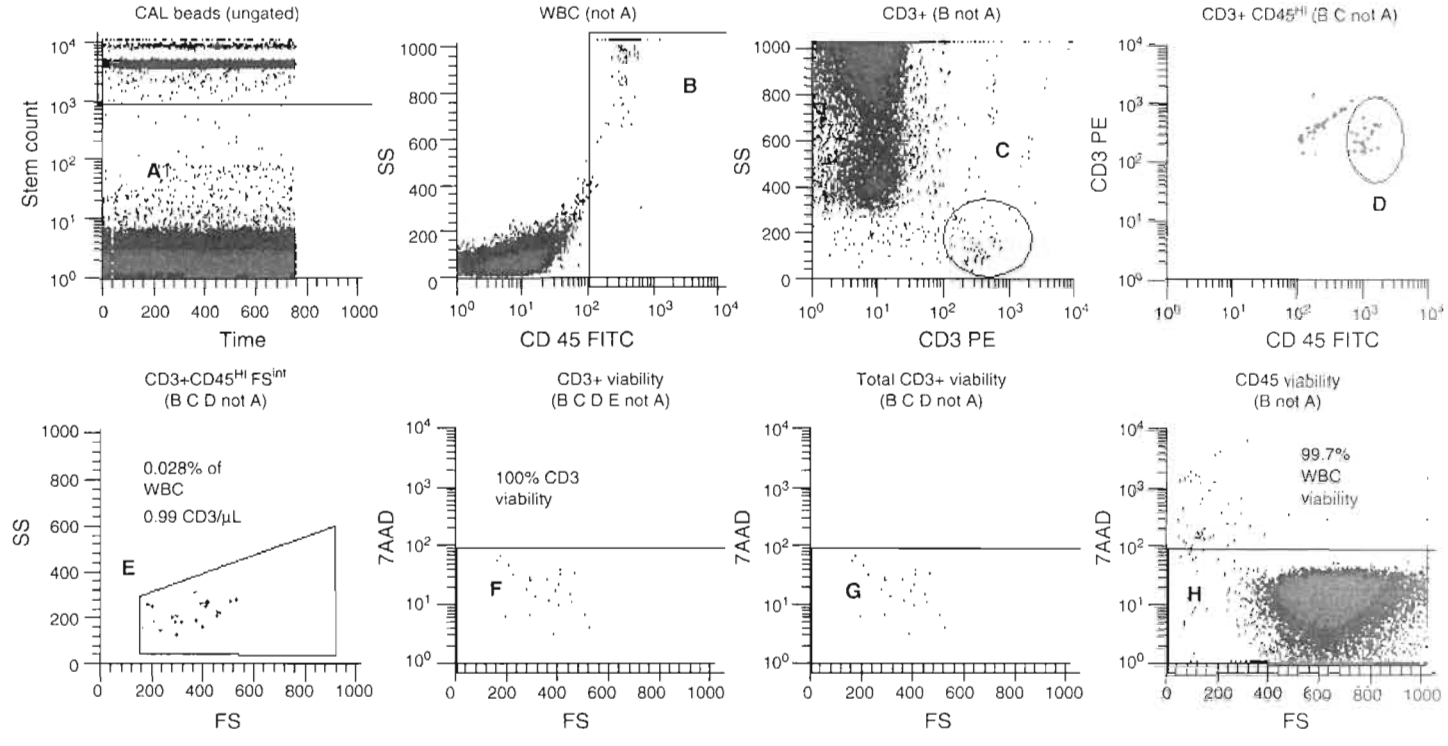

FIGURE 6.15 Detection of CD3+ T cells as rare events in the peripheral blood of a patient on day 0 after completing immunoablative therapy. The same analysis shown in the preceding figure was performed on blood collected immediately after completing immunoablative therapy. Even after acquiring the entire sample, few WBCs were seen (gate B), and the CD3 population did not form a discrete population versus SSc (gate C). The reason for this is apparent in gate D, where T cells with bright CD45 expression are separated from a diagonal of "noise." Following this gating procedure, identified T cells have credible light scatter (gate E) and high viability. The peripheral CD3 count was less than 1 cell/µL. For gates A, G, and H are applied as described in Figure 6.14.

6.16.2 Detection of Circulating Tumor in Cutaneous T-Cell Lymphoma by the Analysis of T-Cell Receptor v-Beta Usage

Cutaneous T-cell lymphoma is a general term that covers several types of T-cell lymphoma of the skin. In a variant known as Sézary syndrome, the presenting features often include widespread redness of the skin (erythroderma) with severe itching. Lymph nodes are enlarged and the malignant T cells found in the skin are also found in the circulation. Because the malignant cells are clonal, they have identical TCR specificities, and therefore, identical v-beta usage. If the v-beta specificity of the skin lesion is known, a circulating tumor can be identified by the excess proportion that they comprise in the peripheral blood. T-cell subsets, roughly corresponding to naïve, memory, effector memory, and late effector cells can be defined by their expression of CD45 isoform [63,64] and CD27 [65–67], CD28 [68,69], or CD62L [70,71]. If the malignant clone is uniquely or predominantly confined to a particular T-cell subset, then examining v-beta usage by the subset provides greater sensitivity to detect the circulating tumor.

In the present example, we examine peripheral blood from a Sézary patient. After separation on a Ficoll–Hypaque gradient, the mononuclear cells were stained in bulk with a cocktail of anti-CD4-PECy7, anti-CD45RA-ECD, and anti-CD27-PC5. The stained cells were aliquoted into 10 microtiter wells (~1 million cells/well), centrifuged, and the supernatant decanted. Eight wells were used to measure 24 v-beta specificities, one well for TCR alpha–beta/gamma–delta and one for the FITC and PE isotype controls. The Beta Mark anti-TCR v-beta staining kit, commercialized by Beckman Coulter, was used for v-beta detection. The v-beta reagents occupied the FITC and PE channels, but covered three v-beta specificities per well. This is possible because only one v-beta specificity is expressed on any given T cell. Thus for a mixture of antibodies to the v-beta families X, Y and Z, X was FITC conjugated, Y was PE conjugated, and Z was a mixture of FITC and PE conjugated antibodies.

We used a *classifier/outcome* gating strategy to examine TCR v-beta usage in T-cell subsets. Primary classifiers are sequential, whereas secondary classifiers branch. In this case, the *primary classifiers* used to identify CD4+ T cells and clean them up were: forward versus log SSc, CD4 versus log SSc, and forward versus log SSc again (Figure 6.16). The secondary classifiers, CD45RA versus CD27 were used to define four subsets within CD4+ cells. The outcomes, namely v-beta specificities, were measured on total CD4+ lymphocytes, and each CD4 subset.

Figure 6.16 details the analysis of 1 of the 10 wells in the panel (v-betas 13.1, 13.6, and 8). The v-beta specificities are given as a percentage of total CD4+ lymphocytes, and of each CD4 subset. The values would be meaningless without reference to expected values derived from a population of healthy control subjects (Figure 6.17). The reason that these ranges are computed and displayed in a logarithmic scale is critical to their interpretation and is explained in detail in Chapter 2, Statistics. From this figure, it is clear that our patient has a marked expansion of v-beta 13.1 CD4+ T cells (12.5% versus the 95th percentile reference range of 2.2–6.6%). Further, the expansion is confined to the CD45RA+ CD27 negative *effector* population, in which they represent 68.6% of all gated cells. This is an important finding, since this patient's

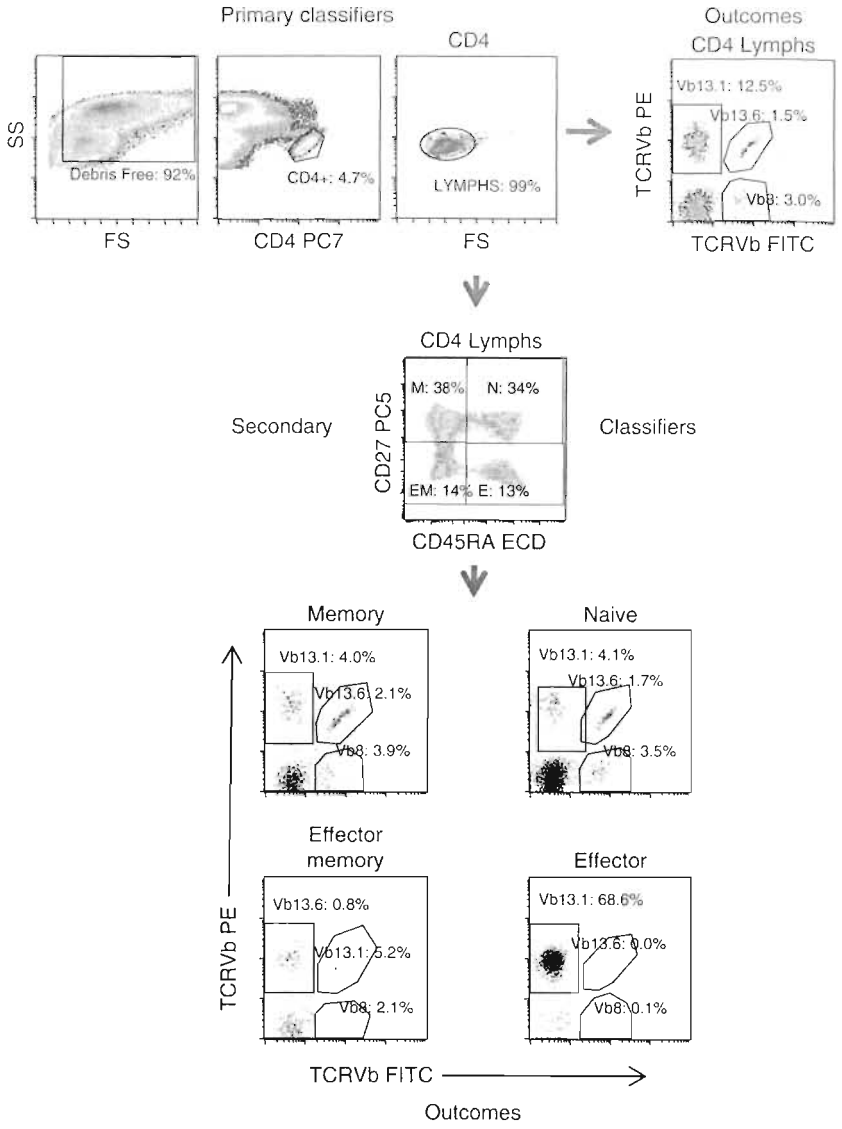

FIGURE 6.16 Use of the classifier/outcome strategy to determine TCR v-beta distribution among subsets of CD4+ lymphocytes. The primary classifiers (light scatter, CD4) are used sequentially to identify a population of CD4+ lymphocytes free of dead cells, debris, and monocytes. The secondary classifiers, CD45RA and CD27 are used to define the CD4 subsets. The outcome parameters (v-beta families) are measured on all the populations defined by the classifiers (total CD4, CD4 subsets). This particular subject, a patient with cutaneous T-cell lymphoma, has a marked expansion in v-beta 13.1, as determined by comparison to expected values defined in Figure 6.17. Virtually, all excess v-beta 13.1+ cells are members of the CD45RA+, CD27− effector subset.

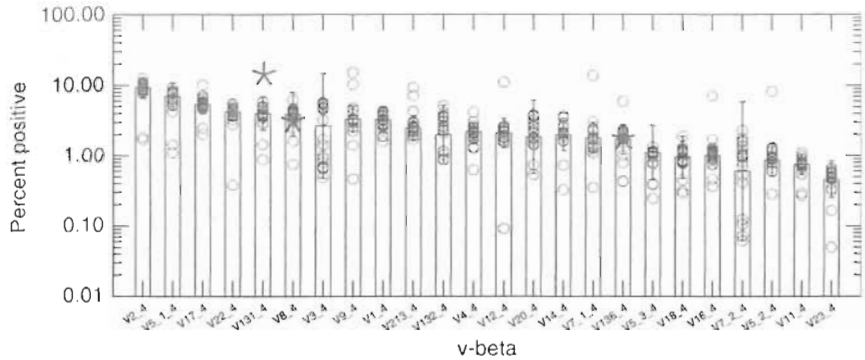

FIGURE 6.17 TCR v-beta usage in healthy adult subjects. The geometric mean values (bars), 95th percentiles (brackets), as well as individual control subject values (open circles) are shown. The proportion of v-beta 13.1, 13.6, and 8 positive CD4 T cells, determined in a peripheral blood sample from a patient with cutaneous T-cell lymphoma (Figure 6.16) are shown with stars. The patient has a significantly higher than expected proportion of v-beta 13.1+ cells, which represents an expansion of the malignant clone. This expansion was even more pronounced in the CD45RA+, CD27− effector subset.

WBC was within normal limits, and circulating Sézary cells are morphologically difficult to differentiate from normal activated T cells. (For more details on Sézary syndrome see Chapter 7.)

This analysis illustrates several principles: (1) Cells were stained in bulk for markers common to all wells; (2) After making a rough cut on forward versus log SSc to eliminate unambiguous debris, CD4+ lymphocytes were distinguished from $CD4^{dim}$ monocytes using CD4 versus log SSc; (3) These CD4+ cells were further cleaned up with an additional forward versus log SSc gate. The rare blast population (high forward scatter) could have been analyzed separately; (4) The analysis was performed according to a *classifier/outcome* strategy. Isotype controls were run on the outcome parameters only, allowing the regions for v-beta populations to be set with confidence; and (5) Time versus forward scatter was examined to detect any irregularities occurring during acquisition (not shown).

6.17 CLOSING REMARKS

This chapter attempts to explain the rudiments of clinical flow cytometry with particular emphasis on avoiding some of the most common pitfalls in instrument setup, experimental design, and data analysis. The most important point that I would like to communicate is that it is the very flexibility of the flow cytometer that makes it dangerous when placed into inattentive hands. Attention to detail, which means proper calibration, proper experimental controls, and a basic knowledge of the workings of the cytometer, all help ensure that the results will be interpretable. Even if you will never operate a flow cytometer, you will almost certainly need to interpret results created by someone else, or even analyze primary data yourself. If you are a laboratorian, it is your responsibility to ask your flow operator how she or he QCs the instrument (and to understand the answer), as well as to learn the controls

and standards appropriate to your experiment. Flow cytometers are almost uniquely robust, such that new tests can be devised as new needs arise. However, the further we move from well-validated clinical assays into the realm of the experimental, the more vigilant we should be. In the words of Albert Einstein, "If we knew what it was we were doing, it would not be called research, would it?"

REFERENCES

1. Sutherland DR, Anderson L, Keeney M, Nayar R, Chin-Yee I. The ISHAGE guidelines for CD34 + cell determination by flow cytometry. International Society of Hematotherapy and Graft Engineering. *Journal of Hematotherapy*, 5(3):213–226, 1996.
2. Lee LG, Chen CH, Chiu LA. Thiazole orange: a new dye for reticulocyte analysis. *Cytometry*, 7(6):508–217, 1986.
3. Hall SE, Rosse WF. The use of monoclonal antibodies and flow cytometry in the diagnosis of paroxysmal nocturnal hemoglobinuria. *Blood*, 87(12):5332–5340, 1996.
4. Voskova D, Schnittger S, Schoch C, Haferlach T, Kern W. Use of five-color staining improves the sensitivity of multiparameter flow cytomeric assessment of minimal residual disease in patients with acute myeloid leukemia. *Leukemia & Lymphoma*, 48(1): 80–88, 2007.
5. Herzenberg LA, Sweet RG, Herzenberg LA. Fluorescence activated cell sorting. *Scientific American*, 234:108–117, 1976.
6. Andreeff M. *Clinical Cytometry*. New York: The New York Academy of Sciences, 1986.
7. Shapiro HM. *Practical Flow Cytometry* (4th edition). Hoboken, NJ: WileySons, 2003.
8. Melamed M, Lindmo T, Mendelsohn M (Editors). *Flow Cytometry and Sorting* (2nd edition). New York: Wiley-Liss, 1990.
9. Givan A. *Flow Cytometry. First Principles*. New York: Wiley-Liss, 1993.
10. Robinson J. *Handbook of Flow Cytometry Methods*. New York: Wiley-Liss, 1993.
11. Snow C. Flow cytometer electronics. *Cytometry Part A: The Journal of the International Society for Analytical Cytology*, 57(2):63–69, 2004.
12. Shapiro HM. The evolution of cytometers. *Cytometry Part A: The Journal of the International Society for Analytical Cytology*, 58(1):13–20, 2004.
13. Pearson T, Galfre G, Ziegler A, Milstein C. A myeloma hybrid producing antibody specific for an allotypic determinant on "IgD-like" molecules of the mouse. *European Journal of Immunology*, 7(10):684–690, 1977.
14. White RA, Mason DW, Williams AF, Galfre G, Milstein C. T-lymphocyte heterogeneity in the rat: separation of functional subpopulations using a monoclonal antibody. *Journal of Experimental Medicine*, 148(3):664–673, 1978.
15. Trowbridge IS. Interspecies spleen-myeloma hybrid producing monoclonal antibodies against mouse lymphocyte surface glycoprotein, T200. *Journal of Experimental Medicine*, 148(1):313–323, 1978.
16. Hammerling GJ, Lemke H, Hammerling U, Hohmann C, Wallich R, Rajewsky K. Monoclonal antibodies against murine cell surface antigens: anti-H-2, anti-Ia and anti-T cell antibodies. *Current Topics in Microbiology and Immunology*, 81:100–106, 1978.
17. Kung P, Goldstein G, Reinherz EL, Schlossman SF. Monoclonal antibodies defining distinctive human T cell surface antigens. *Science*, 206(4416):347–349, 1979.
18. Chow S, Minden MD, Hedley DW. Constitutive phosphorylation of the S6 ribosomal protein via mTOR and ERK signaling in the peripheral blasts of acute leukemia patients. *Experimental Hematology*, 34(9):1183–1191, 2006.

19. Perez OD, Nolan GP. Phospho-proteomic immune analysis by flow cytometry: from mechanism to translational medicine at the single-cell level. *Immunological Reviews*, 210:208–228, 2006.
20. IUIS-WHO Nomenclature Subcommittee. Nomenclature for clusters of differentiation (CD) of antigens defined on human leukocyte populations. *Bulletin of the World Health Organization*, 62:809–811, 1984.
21. Raab L. Simple Complexes Molecular Probes' Zenon technology uses immune complexes to label primary antibodies. *The Scientist*, 16(12):48, 2002.
22. Hamada S, Fujita S. DAPI staining improved for quantitative cytofluorometry. *Histochemistry*, 79(2):219–226, 1983.
23. Park CH, Kimler BF, Smith TK. Comparison of the supravital DNA dyes Hoechst 33342 and DAPI for flow cytometry and clonogenicity studies of human leukemic marrow cells. *Experimental Hematology*, 13(10):1039–1043, 1985.
24. Takahama M, Kagaya A. Hematoporphyrin/DAPI staining: simplified simultaneous one-step staining of DNA and cell protein and trial application in automated cytological screening by flow cytometry. *Journal of Histochemistry and Cytochemistry*, 36(8):1061–1067, 1988.
25. Otto F. DAPI staining of fixed cells for high-resolution flow cytometry of nuclear DNA. *Methods in Cell Biology*, 33:105–110, 1990.
26. Gaforio JJ, Serrano MJ, Algarra I, Ortega E, Alvarez de Cienfuegos G. Phagocytosis of apoptotic cells assessed by flow cytometry using 7-Aminoactinomycin D. *Cytometry*, 49(1):8–11, 2002.
27. Kapuscinski J, Darzynkiewicz Z, Melamed MR. Interactions of acridine orange with nucleic acids. Properties of complexes of acridine orange with single stranded ribonucleic acid. *Biochemical Pharmacology*, 32(24):3679–3694, 1983.
28. Traganos F, Darzynkiewicz Z, Sharpless TK, Melamed MR. Erythroid differentiation of friend leukemia cells as studied by acridine orange staining and flow cytometry. *Journal of Histochemistry and Cytochemistry*, 27(1):382–389, 1979.
29. Bauer KD, Clevenger CV, Williams TJ, Epstein AL. Assessment of cell cycle-associated antigen expression using multiparameter flow cytometry and antibody-acridine orange sequential staining. *Journal of Histochemistry and Cytochemistry*, 34(2):245–250, 1986.
30. Armstrong L, Stojkovic M, Dimmick I, Ahmad S, Stojkovic P, Hole N, Lako M. Phenotypic characterization of murine primitive hematopoietic progenitor cells isolated on basis of aldehyde dehydrogenase activity. *Stem Cells*, 22(7):1142–1151, 2004.
31. Makrigiorgos GM. Detection of lipid peroxidation on erythrocytes using the excimer-forming property of a lipophilic BODIPY fluorescent dye. *Journal of Biochemical and Biophysical Methods*, 35(1):23–35, 1997.
32. Rosati A, Candussio L, Crivellato E, Klugmann FB, Giraldi T, Damiani D, Michelutti A, Decorti G. BODIPY-FL-verapamil: a fluorescent probe for the study of multidrug resistance proteins. *Cellular Oncology*, 26(1–2):3–11, 2004.
33. Lyons AB. Analysing cell division *in vivo* and *in vitro* using flow cytometric measurement of CFSE dye dilution. *Journal of Immunological Methods*, 243(1–2):147–154, 2000.
34. Smith PJ, Wiltshire M, Davies S, Patterson LH, Hoy T. A novel cell permeant and far red-fluorescing DNA probe, DRAQ5, for blood cell discrimination by flow cytometry. *Journal of Immunological Methods*, 229(1–2):131–139, 1999.
35. Coffin RS, Thomas SK, Thomas NS, Lilley CE, Pizzey AR, Griffiths CH, Gibb BJ, Wagstaff MJ, Inges SJ, Binks MH, Chain BM, Thrasher AJ, Rutault K, Latchman DS. Pure populations of transduced primary human cells can be produced using GFP expressing herpes virus vectors and flow cytometry. *Gene Therapy*, 5(5):718–722, 1998.

36. Sorensen SJ, Sorensen AH, Hansen LH, Oregaard G, Veal D. Direct detection and quantification of horizontal gene transfer by using flow cytometry and gfp as a reporter gene. *Current Microbiology*, 47(2):129–133, 2003.
37. Lizard G, Roignot P, Maynadie M, Lizard-Nacol S, Poupon MF, Bordes M. Flow cytometry evaluation of the multidrug-resistant phenotype with functional tests involving uptake of daunorubicin, Hoechst 33342, or rhodamine 123: a comparative study. *Cancer Detection and Prevention*, 19(6):527–534, 1995.
38. Goodell MA, Brose K, Paradis G, Conner AS, Mulligan RC. Isolation and functional properties of murine hematopoietic stem cells that are replicating *in vivo*. *Journal of Experimental Medicine*, 183(4):1797–1806, 1996.
39. Rabinovitch PS, June CH, Grossmann A, Ledbetter JA. Heterogeneity among T cells in intracellular free calcium responses after mitogen stimulation with PHA or anti-CD3. Simultaneous use of indo-1 and immunofluorescence with flow cytometry. *Journal of Immunology*, 137(3):952–961, 1986.
40. Lopez M, Olive D, Mannoni P. Analysis of cytosolic ionized calcium variation in polymorphonuclear leukocytes using flow cytometry and indo-1 AM. *Cytometry*, 10(2): 165–173, 1989.
41. Reers M, Smiley ST, Mottola-Hartshorn C, Chen A, Lin M, Chen LB. Mitochondrial membrane potential monitored by JC-1 dye. *Methods in Enzymology*, 260:406–417, 1995.
42. Bernas T, Dobrucki J. Mitochondrial and nonmitochondrial reduction of MTT: interaction of MTT with TMRE, JC-1, and NAO mitochondrial fluorescent probes. *Cytometry*, 47(4):236–242, 2002.
43. Rice GC, Bump EA, Shrieve DC, Lee W, Kovacs M. Quantitative analysis of cellular glutathione by flow cytometry utilizing monochlorobimane: some applications to radiation and drug resistance *in vitro* and *in vivo*. *Cancer Research*, 46(12, Part 1):6105–6110, 1986.
44. Belloc F, Belaud-Rotureau MA, Lavignolle V, Bascans E, Braz-Pereira E, Durrieu F, Lacombe F. Flow cytometry detection of caspase 3 activation in preapoptotic leukemic cells. *Cytometry*, 40(2):151–160, 2000.
45. Deitch AD, Law H, deVere White R. A stable propidium iodide staining procedure for flow cytometry. *Journal of Histochemistry and Cytochemistry*, 30(9):967–972, 1982.
46. Jacobs DB, Pipho C. Use of propidium iodide staining and flow cytometry to measure anti-mediated cytotoxicity: resolution of complement-sensitive and resistant target cells. *Journal of Immunological Methods*, 62(1):101–108, 1983.
47. Prosperi E, Giangare MC, Bottiroli G. Nuclease-induced DNA structural changes assessed by flow cytometry with the intercalating dye propidium iodide. *Cytometry*, 12(4):323–329, 1991.
48. Ormerod MG, Kubbies M. Cell cycle analysis of asynchronous cell populations by flow cytometry using bromodeoxyuridine label and Hoechst-propidium iodide stain. *Cytometry*, 13(7):678–685, 1992.
49. Darzynkiewicz Z, Traganos F, Staiano-Coico L, Kapuscinski J, Melamed MR. Interaction of rhodamine 123 with living cells studied by flow cytometry. *Cancer Research*, 42(3):799–806, 1982.
50. Murphy RF, Chused TM. A proposal for a flow cytometric data file standard. *Cytometry*, 5(5):553–555, 1984.
51. Fowlkes B, Pardoll D. Molecular and cellular events of T cell development. *Advances in Immunology*, 44:207–264, 1989.
52. Boyum A. Isolation of leucocytes from human blood. Further observations. Methylcellulose, dextran, and ficoll as erythrocyte aggregating agents. *Scandinavian Journal of Clinical and Laboratory Investigation Supplement*, 97:31–50, 1968.
53. College of American Pathologists. College of American Pathologists (CAP) Flow Cytometry—Section II Checklist, edition October 6, 2005.

54. Roederer M. Spectral compensation for flow cytometry: visualization artifacts, limitations, and caveats. *Cytometry*, 45(3):194–205, 2001.
55. Bayer J, Grunwald D, Lambert C, Mayol JF, Maynadie M. Thematic workshop on fluorescence compensation settings in multicolor flow cytometry. *Cytometry Part B, Clinical Cytometry*, 72(1):8–13, 2007.
56. Schwartz A, Marti GE, Poon R, Gratama JW, Fernandez-Repollet E. Standardizing flow cytometry: a classification system of fluorescence standards used for flow cytometry. *Cytometry*, 33(2):106–114, 1998.
57. Mario R. Compensation is not dependent on signal intensity or on number of parameters. *Cytometry*, 46(6):357, 2001.
58. Bagwell CB, Adams EG. Fluorescence spectral overlap compensation for any number of flow cytometry parameters. *Annals of the New York Academy of Sciences*, 677:167–184, 1993.
59. Bagwell CB. HyperLog—A flexible log-like transform for negative, zero, and positive valued data. *Cytometry Part A*, 64A:34–42, 2005.
60. Hultin LE, Matud JL, Giorgi JV. Quantitation of CD38 activation antigen expression on CD8+ T cells in HIV-1 infection using CD4 expression on CD4+ T lymphocytes as a biological calibrator. *Cytometry*, 33:123, 1998.
61. Donnenberg VS, O'Connell PJ, Logar AJ, Zeevi A, Thomson AW, Donnenberg AD. Rare-event analysis of circulating human dendritic cell subsets and their presumptive mouse counterparts. *Transplantation*, 72(12):1946–1951, 2001.
62. Chen YH, Peterson LC, Dittmann D, Evens A, Rosen S, Khoong A, Shankey TV, Forman M, Gupta R, Goolsby CL. Comparative analysis of flow cytometric techniques in assessment of ZAP-70 expression in relation to IgVH mutational status in chronic lymphocytic leukemia. *American Journal of Clinical Pathology*, 127(2):182–191, 2007.
63. Schraven B, Roux M, Hutmacher B, Meuer SC. Triggering of the alternative pathway of human T cell activation involves members of the T 200 family of glycoproteins. *European Journal of Immunology*, 19(2):397–403, 1989.
64. Mason D, Powrie F. Memory CD4+ T cells in man form two distinct subpopulations, defined by their expression of isoforms of the leucocyte common antigen, CD45. *Immunology*, 70(4):427–433, 1990.
65. de Jong R, Brouwer M, Kuiper HM, Hooibrink B, Miedema F, van Lier RA. Maturation- and differentiation-dependent responsiveness of human CD4+ T helper subsets. *Journal of Immunology*, 149(8):2795–2802, 1992.
66. Baars PA, Maurice MM, Rep M, Hooibrink B, van Lier RA. Heterogeneity of the circulating human CD4+ T cell population. Further evidence that the CD4+CD45RA-CD27- T cell subset contains specialized primed T cells. *Journal of Immunology*, 154(1):17–25, 1995.
67. Kuss I, Donnenberg AD, Gooding W, Whiteside TL. Effector CD8+CD45RO-CD27- T cells have signalling defects in patients with squamous cell carcinoma of the head and neck. *British Journal of Cancer*, 88(2):223–230, 2003.
68. Rotteveel FT, Kokkelink I, van Lier RA, Kuenen B, Meager A, Miedema F, Lucas CJ. Clonal analysis of functionally distinct human CD4+ T cell subsets. *Journal of Experimental Medicine*, 168(5):1659–1673, 1988.
69. Monteiro J, Batliwalla F, Ostrer H, Gregersen PK. Shortened telomeres in clonally expanded CD28-CD8+ T cells imply a replicative history that is distinct from their CD28+CD8+ counterparts. *Journal of Immunology*, 156(10):3587–3590, 1996.
70. Currier JR, Stevenson KS, Kehn PJ, Zheng K, Hirsch VM, Robinson MA. Contributions of CD4+, CD8+, and CD4+CD8+ T cells to skewing within the peripheral T cell receptor beta chain repertoire of healthy macaques. *Human Immunology*, 60(3):209–222, 1999.
71. Hamann D, Baars PA, Rep MH, Hooibrink B, Kerkhof-Garde SR, Klein MR, van Lier RA. Phenotypic and functional separation of memory and effector human CD8+ T cells. *Journal of Experimental Medicine*, 186(9):1407–1418, 1997.